



Analysis of Fast-Response NO_x Measurements at Heathrow Airport

Document Control

Client	Defra	Principal Contact	Rob Arnold
---------------	-------	--------------------------	------------

Job Number	J598
-------------------	------

Report Prepared By:	Prof. Duncan Laxen and Dr Ben Marner (AQC) Dr David Carslaw (Institute for Transport Studies, University of Leeds) Dr Karl Ropkins (Institute for Transport Studies , University of Leeds)
----------------------------	--

Document Status and Review Schedule

Issue No.	Report No.	Date	Status	Reviewed by
1	598/1/D1	17 April 2007	Draft 1	Stephen Moorcroft (AQC)
2	598/1/F1	22 May 2007	Final	Stephen Moorcroft (AQC)
3	598/1/F2	18 June 2007	Final	Stephen Moorcroft (AQC)

This report has been prepared by Air Quality Consultants Ltd on behalf of the Client, taking into account the agreed scope of works. Unless otherwise agreed, this document and all other Intellectual Property Rights remain the property of Air Quality Consultants Ltd.

In preparing this report, Air Quality Consultants Ltd has exercised all reasonable skill and care, taking into account the objectives and the agreed scope of works. Air Quality Consultants Ltd does not accept any liability in negligence for any matters arising outside of the agreed scope of works.

Air Quality Consultants Ltd
23 Coldharbour Road, Bristol BS6 7JT Tel: 0117 974 1086
12 Airedale Road, London SW12 8SF Tel: 0208 673 4313
aqc@aqconsultants.co.uk

Contents

1	Introduction	2
2	Methodology	4
3	Results and Discussion	10
4	Conclusions and Recommendations	32
	References	34
	Acknowledgements	34
	Appendix A - Isolation of Peaks from Baseline	35
	Appendix B – Semi-Automated Alignment of NO _x Peaks to Aircraft Departures on Runway 027R	37
	Appendix C - Automated Alignment of NO _x Peaks to Aircraft Departures	39
	Appendix D – Identification of NO _x Peaks During Take-offs on Runway 027L	41
	Appendix E – Daily Plots of 10-second NO _x Concentrations and 15-minute Wind Speed and Wind Directions at LHR2	44
	Appendix F – Daily Plots of 10-second NO _x Concentrations and Calculated Baseline at LHR2 and Measured Background at LHR8 (Oaks Road)	52

1 Introduction

- 1.1 Air Quality Consultants Ltd and Dr David Carslaw of the Institute for Transport Studies, University of Leeds, have been commissioned by Defra to analyse fast-response nitrogen oxides (NO_x) data collected at the LHR2 monitoring site at Heathrow Airport. This monitoring site is located on the northern boundary of the airfield, 180 m from the centre of the northern runway, and 1600 m from the southern runway (Figure 1). With southwesterly winds LHR2 is downwind of aircraft departing to the west on the northern runway (027R). It is also downwind of the Central Terminal.
- 1.2 The fast-response NO_x data were collected as part of the Project for the Sustainable Development of Heathrow (PSDH), funded by DfT (DfT, 2006). A sample of the results was presented in the PSDH report. This sample showed that when the northern runway, 027R, was used for departures (to the west), large, short-lived, peaks of nitrogen oxides, which could rise to over 1,000 µg/m³, were observed. These peaks were not present when the runway use changed to departures on the southern runway 027L. It was clear that discrete plumes of several tens of seconds duration were being detected at LHR2. These peaks are sufficiently discrete to be linked to individual aircraft movements, but no further analysis was carried out as part of the PSDH.
- 1.3 The overall aim of the current project is to analyse the fast-response NO_x data in greater detail, in order to provide a better understanding of aircraft emissions and their dispersion from source to receptor. To achieve this aim, the data collected over the one month period, 19 October to 15 November 2005, have been analysed in relation to a number of meteorological factors and linked to detailed aircraft movement data.
- 1.4 This report expands on the previous analysis of the rates of aircraft emissions and subsequent dispersion, undertaken as part of the PSDH. The findings should help the formulation of improved modelling of aircraft emissions at airports.

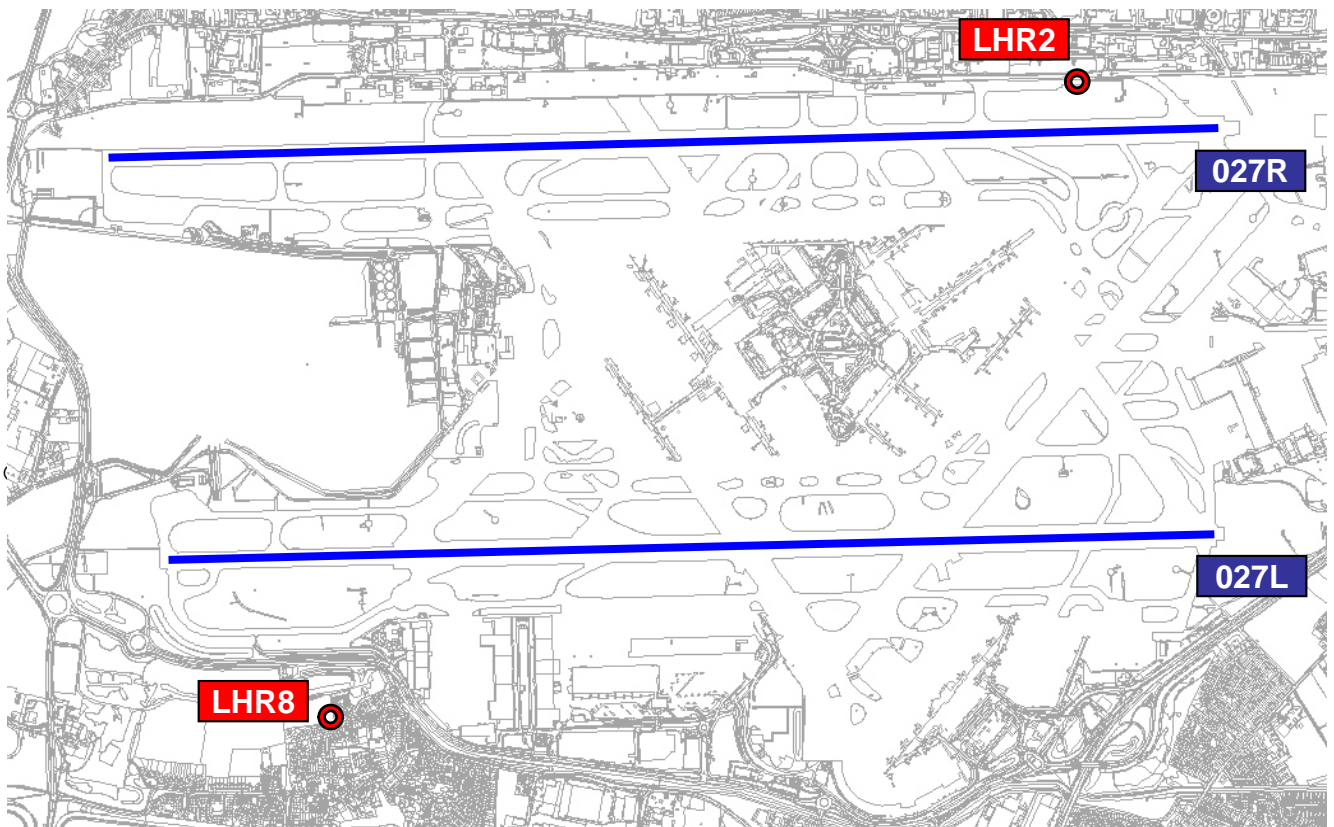


Figure 1 Location of Monitoring Sites and Runways at Heathrow Airport.

2 Methodology

Data Sources

NO_x Concentrations

- 2.1 Measurements of NO_x are carried out routinely at the Heathrow LHR2 site by AEA Energy and Environment on behalf of BAA. Monitoring is carried out using an API single-chamber chemiluminescent analyser (M200). The principle of operation requires the instrument to switch between measurements of nitric oxide (NO) and NO_x. Nitrogen dioxide (NO₂) concentrations are then calculated by subtraction (NO_x – NO). The instrument is operated to QA/QC standards that are identical to those used in the UK Automatic Urban and Rural Network (AURN) (www.airquality.co.uk). The data are processed within the instrument to provide 15-minute mean concentrations.
- 2.2 Additional measurements of NO_x were carried out by AEA Energy and Environment at the LHR2 site between 19 October and 15 November 2006. This monitoring was carried out on behalf of BAA, and was intended to inform the PSDH report. These measurements were carried out using an Environnement SA dual-chamber chemiluminescent analyser (AC31M), which is capable of measuring NO_x and NO simultaneously, with the NO₂ once again calculated by difference. The analyser was calibrated using the same standards as for the single chamber analyser, and once again, both the operation and QA/QC conformed to the procedures used in the AURN.
- 2.3 The dual-chamber instrument was set up to operate with a much faster response time than the single-chamber instrument, with the intent that individual NO_x peaks could be identified. It was set up to record 10-second spot values, with a T90 response time¹ of about 60 seconds.
- 2.4 Unfortunately, the calculated NO₂ measurements from the dual-chamber analyser appeared anomalous, and it was not possible to identify the cause of the error. These data were therefore discarded, and this report focuses on the NO_x measurements alone. In order to provide a further data quality check, a comparison of the NO_x measurements made by the single and dual-chamber instruments was carried out, and is provided in Section 3 of this report.

¹ T90 defines the response time for the instrument to rise from zero to 90% of Full Scale.

Meteorological Data

- 2.5 Meteorological data have been obtained from two sources. One is the output of the official Met Office monitoring site at Heathrow Airport. Amongst other parameters, this measures wind speed and direction at the standard 10 m height at a location on the northern boundary of the airfield above the tunnel to the Central Terminal area. The measurements are made with a cup anemometer and wind vane, and recorded as 1-hour mean values. The second is the output of a sonic anemometer located on the roof of the LHR2 monitoring station, with 15-minute mean values being recorded on a data logger. The anemometer is around 1 m above the roof of the monitoring station and around 4 m above the ground.
- 2.6 The data from the Met Office site have subsequently been processed through the urban meteorological pre-processor within the ADMS modelling package, to provide the Monin Obukov length (L_{MO}) and the estimated boundary layer height (h). These provide a measure of atmospheric stability, defined as h/L_{MO} .

Aircraft Departure

- 2.7 Information on aircraft arrivals and departures was purchased from NATS for the 4 week period corresponding to the fast-NOx measurement data. The information provided details as follows:
- for take-offs: the 'airborne time' in GMT to the nearest second, which is the time the aircraft wheels leave the ground, which is around 30 seconds after start of roll;
 - for landings: the 'threshold time' in GMT to the nearest second, which is the time when an arrival crosses the beginning of that portion of the runway usable for landing. In nearly all cases, arriving aircraft are still airborne when crossing the runway threshold, touching down typically 400 m down the runway at a point due south of the LHR2 monitoring site;
 - the wake vortex category of the aircraft: Heavy, Upper, Medium, Light and Small (see Table 1);
 - the call sign for the flight, which allows the carrier to be identified (only for departures);
 - the aircraft type.

Table 1 Aircraft Type by Wake Vortex Category

	Heavy	Upper	Medium	Light	Small
Aircraft Types	A330-200	B750-200	A319	BE20	CL60
	A330-300	B750-300	A320	BE40	CRJ2
	A340-200	DEF	A320-100	BE9L	CRJ7
	A340-300		B463	C500	E145
	A340-600		B730-300	C525	F50
	A306		B730-400	C550	F70
	A30B		B730-500	C560	F900
	A310		B730-600	C56X	FA50
	B740-100		B730-700	C750	GLF4
	B740-200		B730-800	C328	GLF5
	B740-300		B730-900	F2TH	
	B740-400		E135	FA20	
	B740-S		F100	GLEX	
	B760-200		MD-81	H25B	
	B760-300		MD-82	LJ31	
	B770-200		MD-87	LJ35	
	B770-300		MD-88	LJ45	
	DC10		MD-90	LJ60	
	IL96		RJ1H	PA31	
	MD11		RJ85		
	MD81		T154		

Aircraft Emissions

- 2.8 Information on aircraft NO_x emissions has been obtained from the ICAO database for individual engine types (www.caa.co.uk). For a particular aircraft type the engine can vary from one carrier to another, and even within a carrier there may be more than one engine type in use for a particular aircraft frame. Information on the engines used by the different operators using Heathrow has been obtained from work carried out by AEA Energy and Environment on behalf of BAA, as part of the compilation of a detailed emission inventory for the airport. Where a particular operator used a particular aircraft type with more than one engine type, then a weighted average was used to calculate emissions for that operator / aircraft type.

Data Processing

Isolation of Concentration Peaks from the Baseline

- 2.9 The NO_x peaks were isolated from the baseline using a method developed and written in Visual Basic, details of which are provided in Appendix A. This package also allowed overlapping peaks to be separated. For each peak, information was provided on peak height (above baseline) and peak area.

Identification of 'Other Airport' Component

2.10 The baseline identified as described above includes background concentrations being brought into the Heathrow area together with emissions from elsewhere on the airport, other than aircraft departing on runway 027R. This 'other airport' component will include emissions from aircraft auxiliary power units (APUs), aircraft starting at stands, aircraft taxiing, airside vehicles and landside vehicles accessing the Terminals. Background concentrations have been determined using the results from the monitoring site LHR8 (Oaks Road) located to the south of the airport (Figure 1). The 'other airport' component is thus baseline minus background.

Assigning Concentration Peaks to Aircraft Departures

2.11 Aircraft departures on runway 027R were recorded in the NATS database as airborne time to the nearest second, while NO_x concentrations were recorded as 10-second means. Departures occur up to one a minute during peak periods, or with a two minute gap following departure of a Heavy aircraft, due to the need for subsequent aircraft to avoid the wake of the previous departure. Given the high frequency of departures, the matching of concentration peak to a particular aircraft departure is not straightforward, especially as:

- the section of runway from which emissions give rise to peak concentrations will vary depending on wind direction. The time the aircraft passes this section of runway in relation to the stated airborne time will thus vary from day to day. It will also vary in relation to the aircraft types, as Heavy aircraft will spend longer on the ground during take-off roll;
- there is a delay introduced by the time taken for the emissions to travel from the runway to the monitor, which will depend on wind direction and wind speed;
- a further delay is introduced by the length of inlet tube to the monitor;
- times are recorded on two separate clocks (by NATS and the internal logger at LHR2), which might not be precisely synchronised.

For these reasons the measured concentration peak for a particular aircraft may occur before or after the nominal airborne time for that aircraft, although it is more likely to occur after. The aim of the matching process is to assign a particular aircraft departure to each of the concentration peaks.

Semi-Automated Assignment of Concentration Peaks to Aircraft Departures on 027R

2.12 From an initial examination of plotted NO_x data on a fine time resolution, together with the record of the airborne time for Heavy aircraft, it was evident that the movements could easily be linked to a

peak (see example in Figure 2). The first stage of the matching thus relied on a visual examination of the data to bring the two corresponding time series within +/- 30 seconds of one another. The second stage was an automated process which effectively “snapped” each take-off to the nearest corresponding concentration peak. Full details are provided in Appendix B.

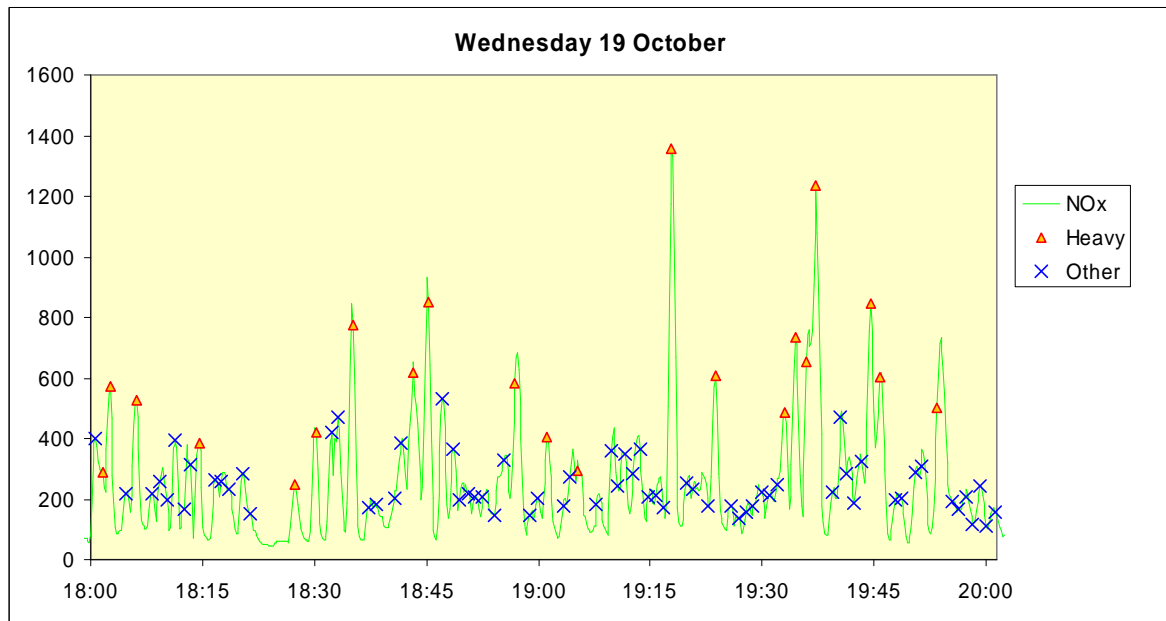


Figure 2 Example of Concentration Peaks and Aircraft Departures on Runway 027R (Prior to Peak Matching). NO_x concentrations in µg/m³

Automated Assignment of Concentration Peaks to Aircraft Departures

- 2.13 The semi-automated approach is relatively time consuming and would be difficult to extend to a larger dataset. There is also a risk that it would not be fully reproducible if repeated, although this is not considered to be a major source of error given the clarity of the linkage between large peaks and take-offs of Heavy aircraft. An alternative approach is to use some sort of algorithm to match the peaks to aircraft departures. This is a common problem addressed in chromatography and mass spectrometry.
- 2.14 Correlation Optimised Warping (COW) is one of a number of ‘warping’ techniques developed to align comparable data sets subject to non-linear time off-setting. This approach has been applied to the alignment of NO_x peaks and aircraft departure data. Details are provided in Appendix C. This matching process has been applied to westerly take-offs on both the northern (027R) and southern (027L) runways. Peaks due to the latter are far less distinct, but matching was still considered possible. A check was carried out to ensure that the peaks being identified at LHR2

during periods of departures on 027L were not due to arrivals on 027R. The evidence was that the peaks were more likely to be due to departures than arrivals (Appendix D).

3 Results and Discussion

- 3.1 This section sets out the results and their analysis. The 10-second NO_x concentrations and 15-minute wind data are shown graphically for the full 28 days in Appendix E. The outcome of the data processing has been to produce 5,617 aircraft departures on 027R matched to concentration peaks at LHR2. Datasets suitable for analysis are available on 20 of the 28 days for which data were available and these are identified in Appendix E. These are days when the wind was blowing from the runway towards LHR2 and take-offs were to the west on 027R (the airport operates a westerly preference for take-offs. Thus even with easterly winds take-offs will be to the west during the daytime when the easterly (tailwind) component is less than 5 knots (about 2.6 m/s).
- 3.2 NO_x concentrations separated into peaks, baseline and background values are shown for each of the days in Appendix F.
- 3.3 A number of data checks have been carried out and these are described first, before examining the factors influencing the concentrations.

Data Checks

Wind Data

- 3.4 A comparison was made between wind direction and wind speed measured by the Met Office at the official Heathrow weather station and the values measured by AEA Energy and Environment at the LHR2 site (Figures 3 and 4). It is clear that there is close agreement between the two datasets, although with some evidence of higher wind speeds at the Met Office site. This is to be expected, as the latter is at 10 m above the ground, while the LHR2 anemometer is 4 m above the ground.
- 3.5 For the purposes of this study it is considered most appropriate to use the LHR2 data, as the values are more directly related to the wind behaviour in the vicinity of this site.

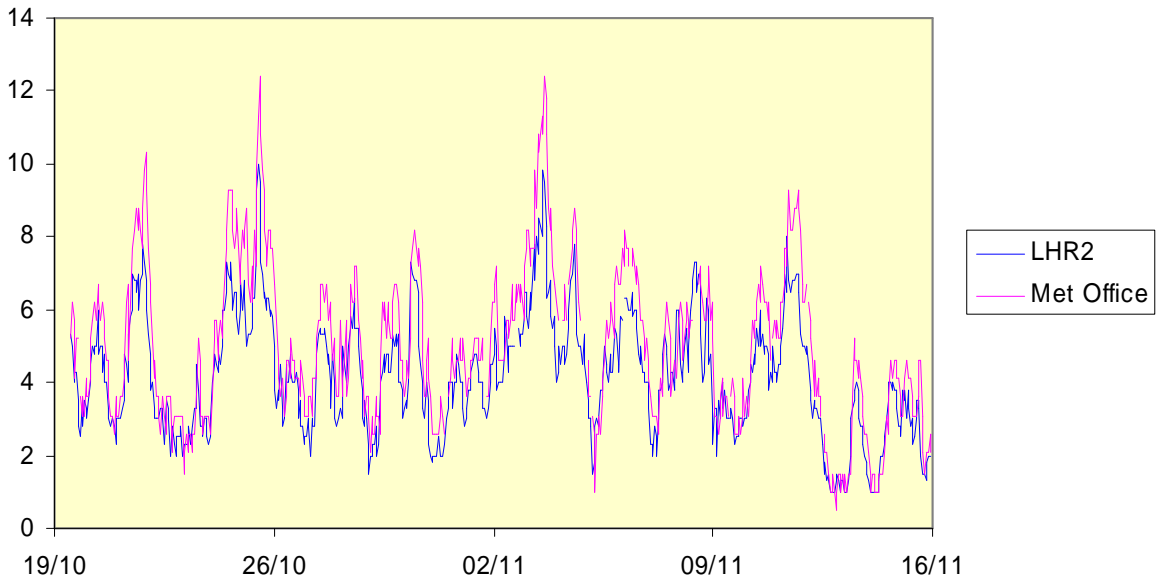


Figure 3 Wind Speed at LHR2 and Heathrow Met Office Sites 19 October to 15 November 2005. Wind speed in m/s.



Figure 4 Wind Direction at LHR2 and Heathrow Met Office Sites 19 October to 15 November 2005. Wind Direction in Degrees.

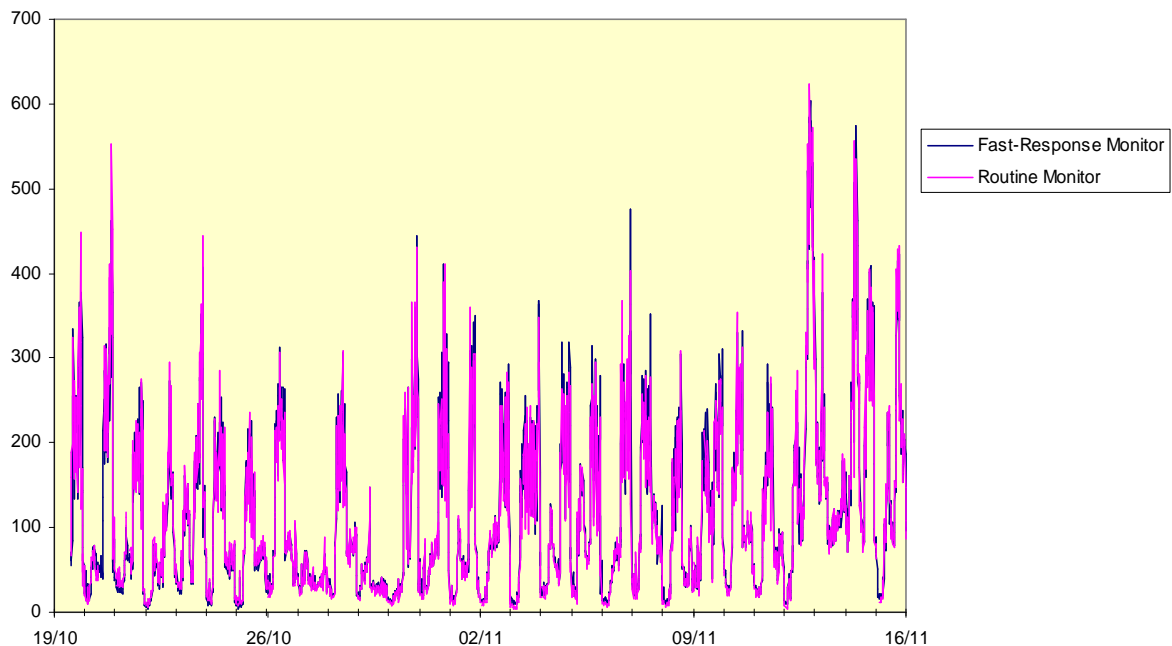


Figure 5 15-minute NO_x Concentrations (mg/m³) Measured with Fast-Response and Routine Monitors at LHR2, 19 October to 15 November 2005.

NO_x Data

- 3.6 LHR2 is a long-running monitoring site that uses a single chamber instrument to routinely measure NO_x, recording the values as 15-minute concentrations. The 10-second data from the fast-response instrument have been worked up into 15-minute concentrations and are shown against the 15-minute values from the routine monitor in Figure 5. There is good agreement between the two monitors giving confidence in the fast-response data.

Peak Assignment to Aircraft Departures on 027R

- 3.7 An indirect check on the two methods of assignment has been carried out by comparing the peak height statistics for different aircraft types derived using the semi-automated procedure and the Correlation Optimised Warping procedure. Peak heights are shown as a mean and 95th percentile uncertainty interval for 14 aircraft types in Figure 6. Overall there is excellent agreement between the two methods, with the semi-automated method showing a slightly narrower uncertainty interval, suggesting it is slightly more robust than the Correlation Optimised Warping method. The results from the semi-automatic matching have thus been used in all subsequent analyses. The comparison confirms, nevertheless, that the Correlation Optimised Warping method will produce acceptable results for similar campaigns over a longer period.

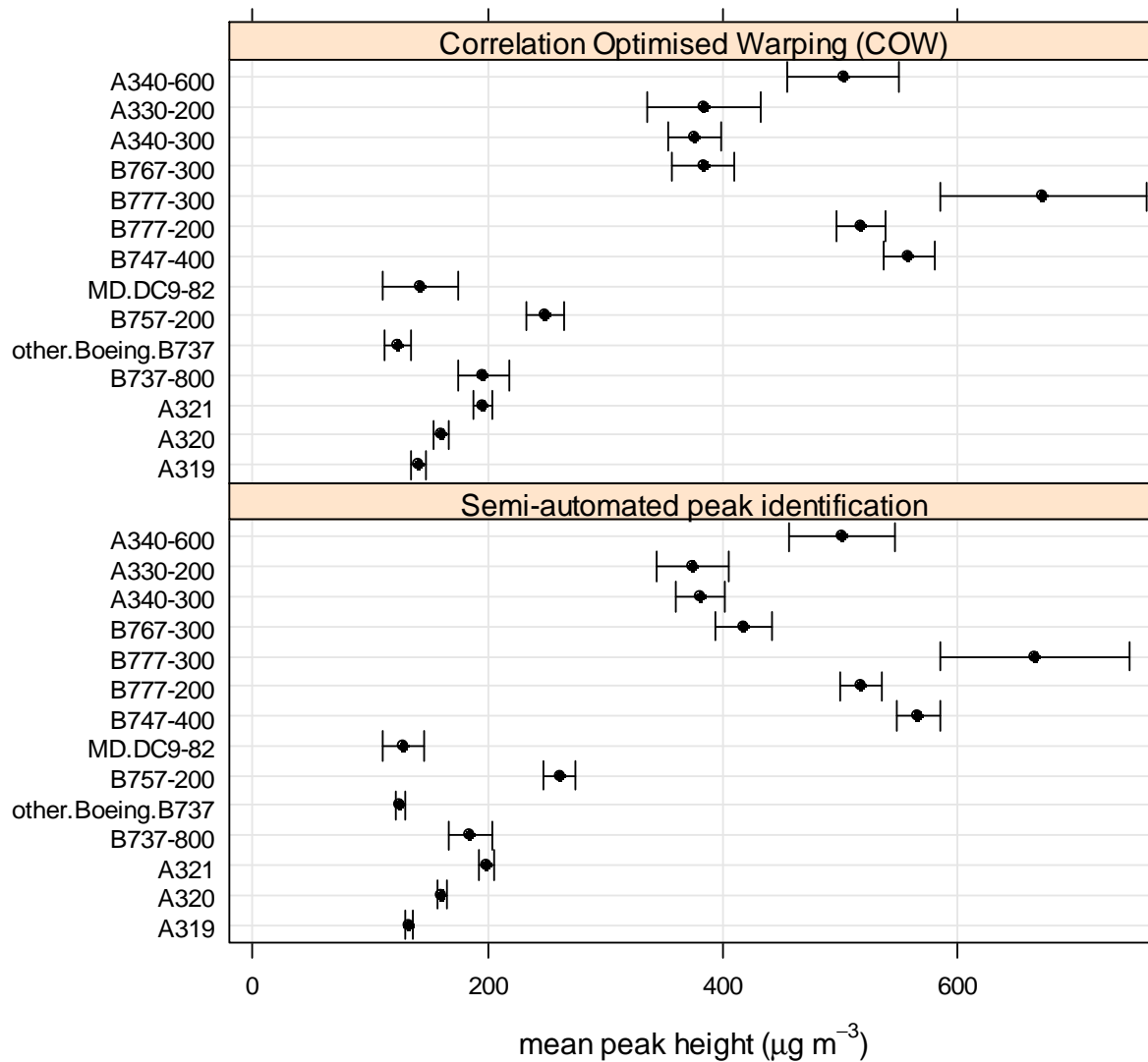


Figure 6 Mean NO_x Peak Height by Aircraft Type, as Identified by the Automated Correlation Optimised Warping Procedure and the Semi-Automated Methodology.

Daily Data Sets

3.8 The full set of 10-second NO_x data is shown a series of Figures in Appendix E, together with the 15-minute wind direction and wind speed data for the monitor at LHR2. This shows the clear influence of aircraft departures on 027R to measured NO_x concentrations. Particularly evident is the switch between the northerly and southerly runways at around 1500h local time (there was a change from summer to winter time on 30 October; prior to this time the switch was at 1400h GMT). This is varied from week to week, with morning departures on 027R for one week and afternoon departures on 027R the next week.

3.9 The winds were predominantly from the southwest (195-255°) during the monitoring period (Figure 7), with moderate speeds predominating (2-7 m/s) (Figure 8). The joint frequency distribution (Figure 9) shows that the highest wind speeds, i.e. those >7 m/s, are associated with winds from the southwest.

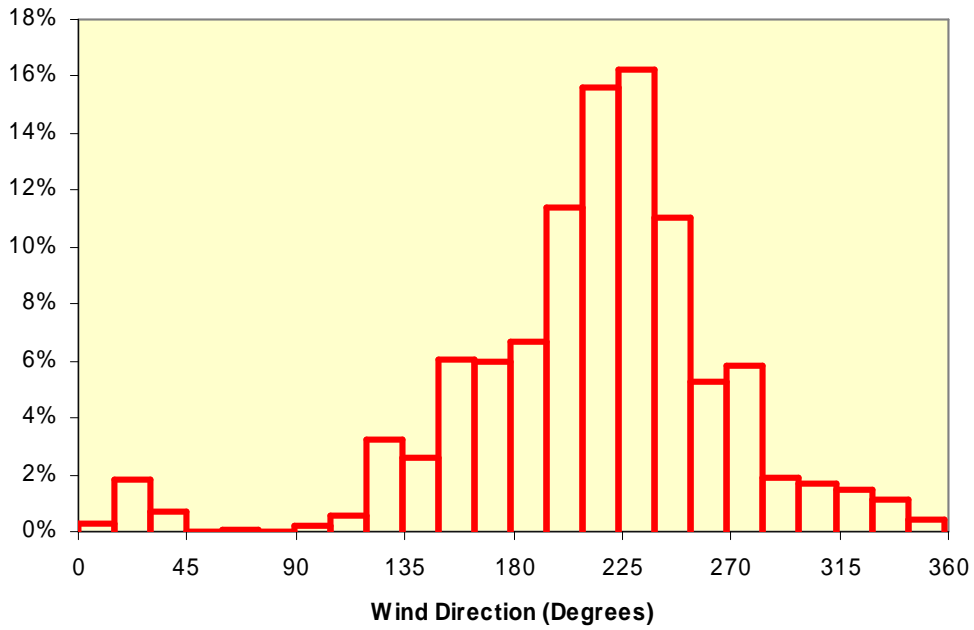


Figure 7 Frequency Distribution of 15-Minute Wind Directions at LHR2, 19 October to 15 November 2005

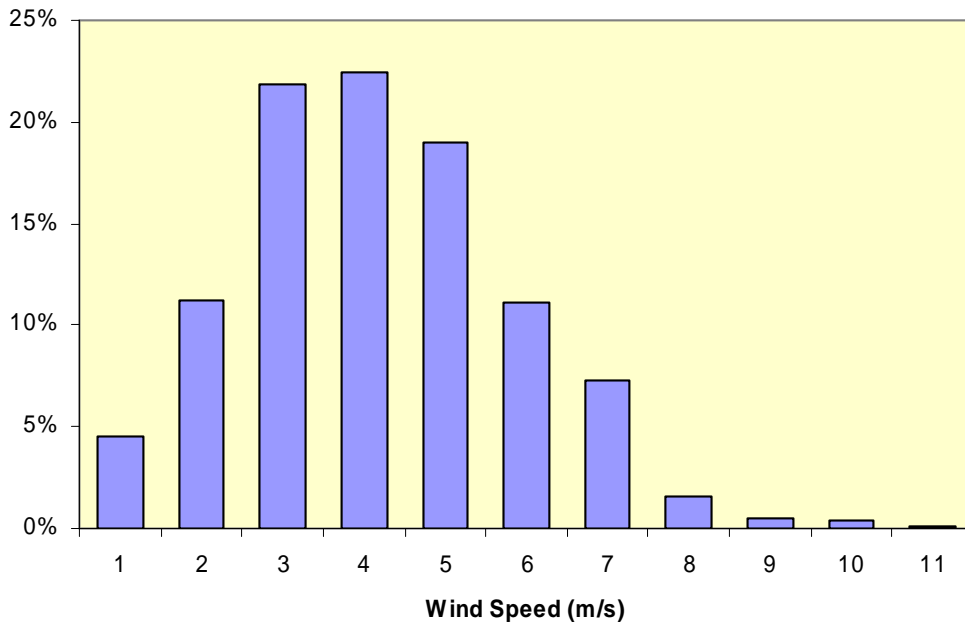


Figure 8 Frequency Distribution of 15-Minute Wind Speeds at LHR2, 19 October to 15 November 2005

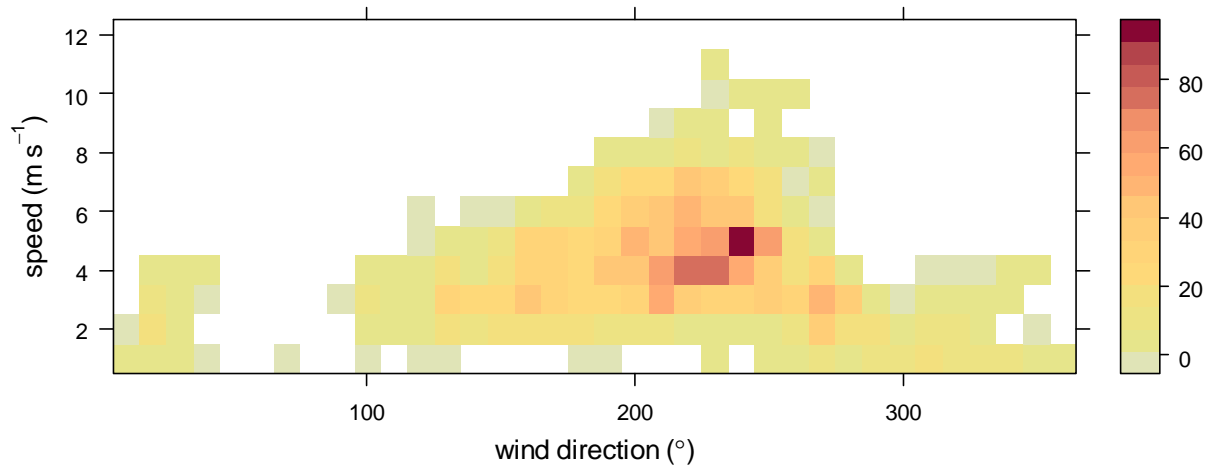


Figure 9 Joint Wind Speed – Wind Direction Frequency Distribution at LHR2, 19 October to 15 November 2005

3.10 Consideration has been given to whether peak height or peak area might be a better indicator of the total NO_x concentration associated with an aircraft plume. The evidence is that the shape of the peak is essentially independent of the peak height (Figure 10), and as a consequence, there is a very close relationship between peak height and peak area (Figure 11). It is thus considered appropriate to focus the analysis on the peak NO_x concentrations.

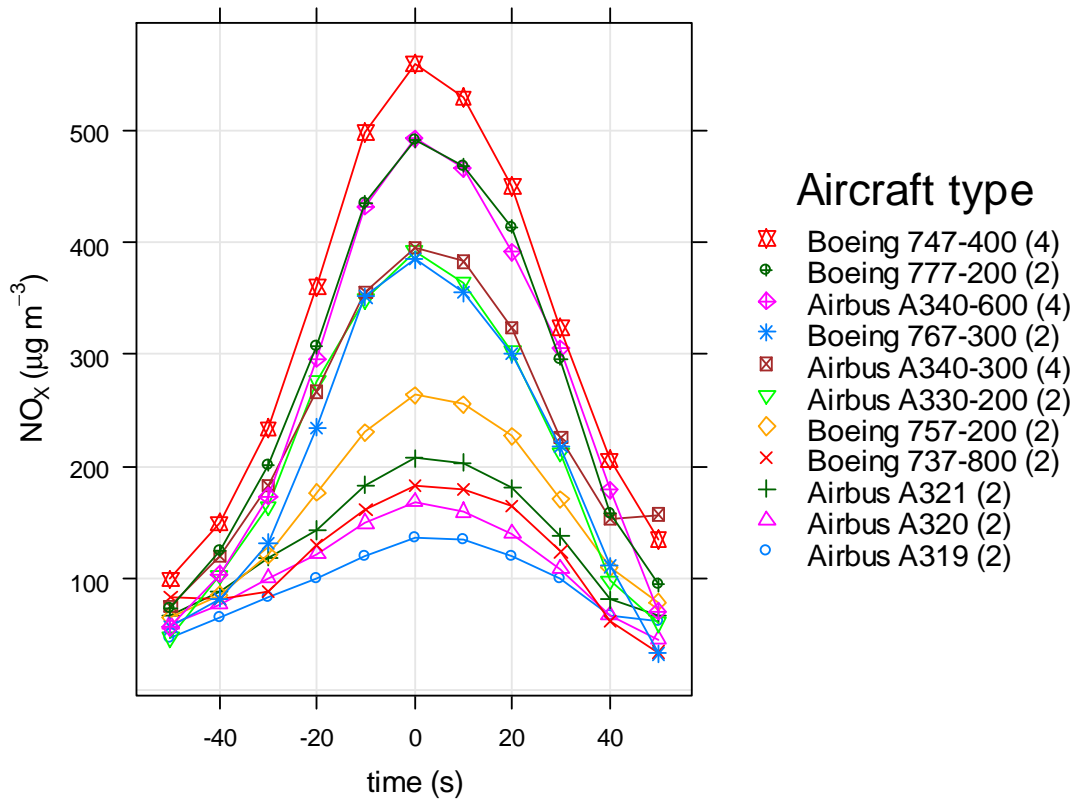


Figure 10 Peak Shape Averaged by Aircraft Type Across Full Dataset. The values in brackets are the number of engines for each particular aircraft type.

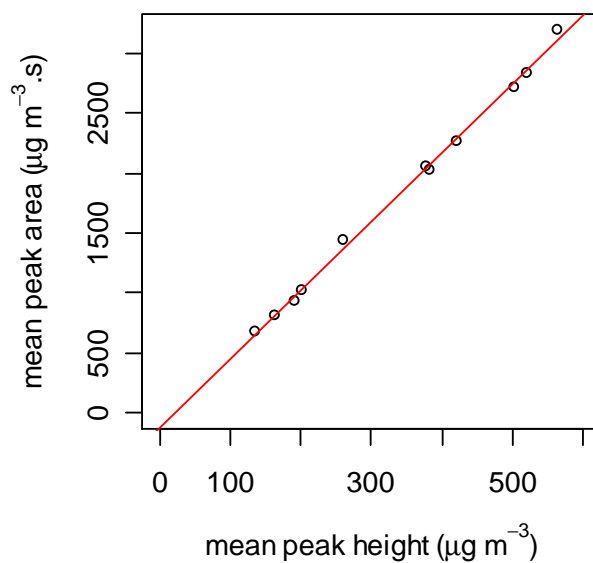


Figure 11 Relationship Between Mean Peak Height and Peak Area for Different Aircraft Types.

Factors Influencing Peak Concentrations

Overview

3.11 The peaks extracted semi-automatically have been compared with several other variables that might be expected to affect them. Figure 12 shows a 'pairs plot' of 1000 peaks randomly selected from the dataset (a sub sample, approximately 20%, has been taken in order to improve the clarity of the plots – all subsequent analyses are based on the full data set of extracted peaks). The histograms set out on the diagonal show the distribution of data for each variable. Considering the top row, the Figure shows the dependence of peak height on each of the other variables. It shows for example, that peak height is almost invariant with wind speed. Also evident is the dependence of wind speed and atmospheric stability on time of day, with wind speed higher during daylight hours, when the atmosphere less stable. The factors influencing peak height are considered further below. In all the following analyses the peaks are shown with the baseline removed.

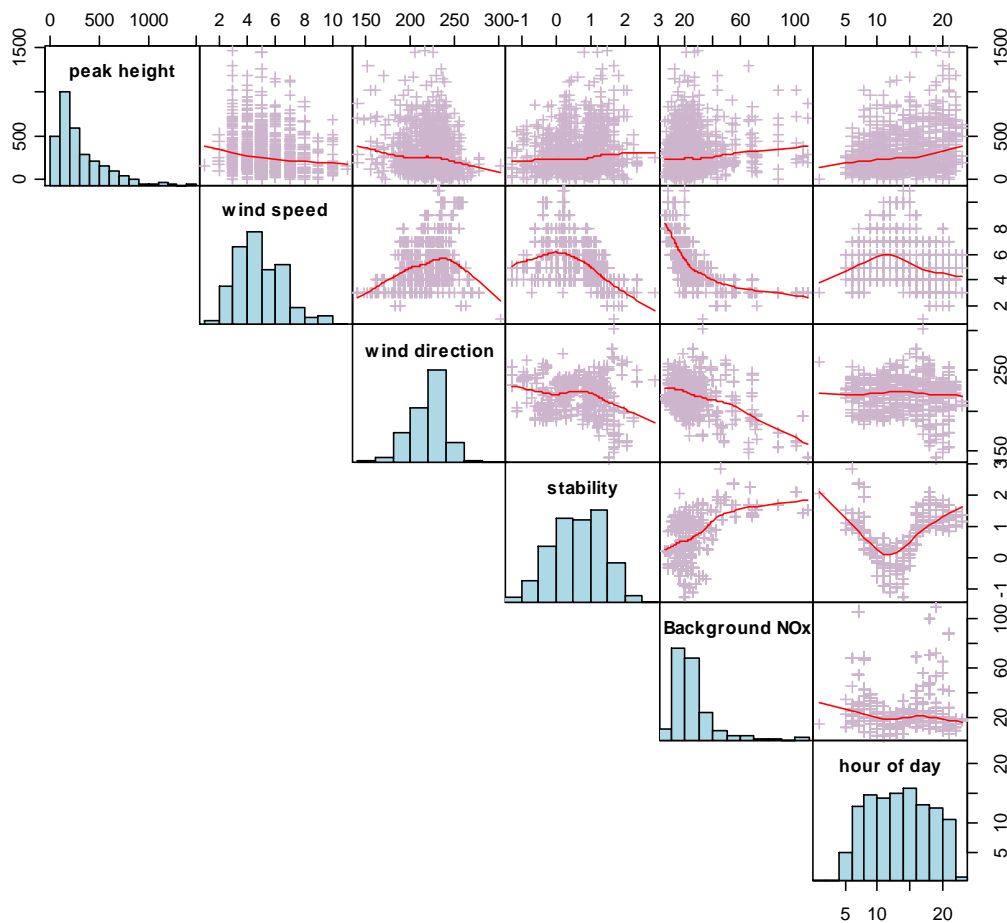


Figure 12 Pairs Plot of NOx Peak Height and Other Variables. Based on a random subsample of 1000 data points. The red line is the best fit line (Loess - locally weighted polynomial regression), to highlight the relationships between variables.

Role of Wind Direction

3.12 Peak concentrations are only observed at LHR2 when the wind is blowing from the south-southeast through to the west (Figure 13 and 14). These directions are associated with emissions from aircraft departing on runway 027R. The two ends of the runway are roughly 115° and 265° in relation to the monitoring site (Figure 1). Winds will blow from the eastern end of the runway on those occasions when wind speeds are low ($<2.6\text{m/s}$) and the 'westerly preference' is operating despite the easterly wind. There is no strong dependence of peak height on wind direction. The dip with westerly winds, i.e. $>240^{\circ}$, is to be expected, as the emissions will be arriving from aircraft at a point well down the runway. Consequently, there will have been a longer travel time, allowing greater dispersion and dilution. In addition, the emission density per metre length of runway will be lower at the western end of the runway due to the greater velocity of the aircraft at this point of take-off, although conversely, with an acute angle to the runway, the emissions from a longer length of runway will contribute to the plume measured at LHR2. The shortest travel time for the emissions will be with southerly winds, around 180° . A little surprisingly, there is no strong evidence of higher concentrations associated with southerly winds than with more westerly winds (say $210\text{-}220^{\circ}$), which will have experienced a longer travel distance. There is some evidence though of slightly higher concentrations associated with south-southeasterly winds. These winds are of lower speed than with the more westerly winds (due to the fact that they are tail-winds, and if stronger, the take-off would be changed to 09R, to the east), however this is not likely to be the explanation, as the influence of wind speed suggests lower peaks at the lowest wind speeds (see next section). The other factor is that aircraft are at the start of roll, which gives rise to a greater emission density, i.e. emissions per length of runway are at their highest. There will also be less influence of aircraft wake vortices on dispersion.

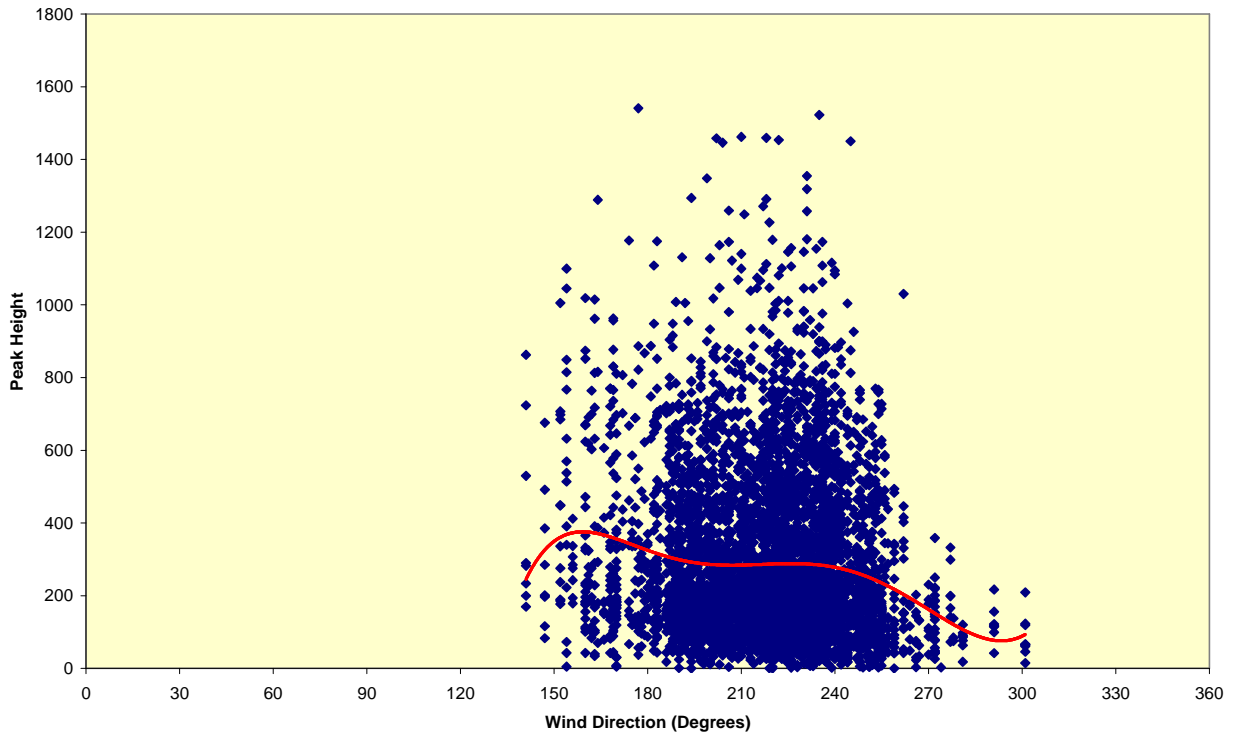


Figure 13 10-Second NO_x Concentrations (mg/m³) at LHR2 vs Wind Direction. The line is a polynomial best fit.

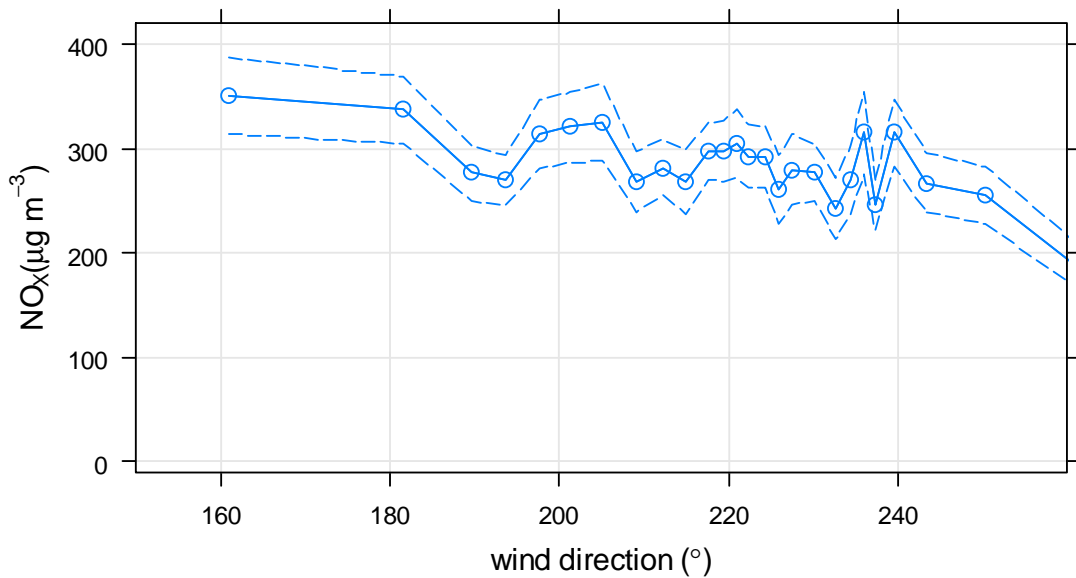


Figure 14 Mean 10-Second NO_x Concentrations at LHR2 vs Wind Direction. The values shown are the mean peak heights and 95th percentile limits.

Role of Wind Speed

3.13 The dependence of peak height on wind speed has been examined with particular attention, as earlier work as part of PSDH identified that emissions from aircraft do not undergo the same sort of dilution as ground-level sources. It was found that concentrations either tended to increase with wind speed or be largely invariant with wind speed. The current dataset confirms the weak relationship between peak height and wind speed, especially when contrasted with the strong dependence of background concentrations on wind speed (Figure 12).

3.14 Figure 15 shows a box and whiskers plot of peak heights for all aircraft types as a function of wind speed. This shows an increase in peak heights to 3 m/s, then a slow decline. These features are similar to those expected for an elevated source, resulting either from release of material at height or through dispersion following a rise due to buoyancy. Given that aircraft engine exhaust plumes exit aircraft close to the ground, it is likely that buoyancy effects are an important feature of the relationship.

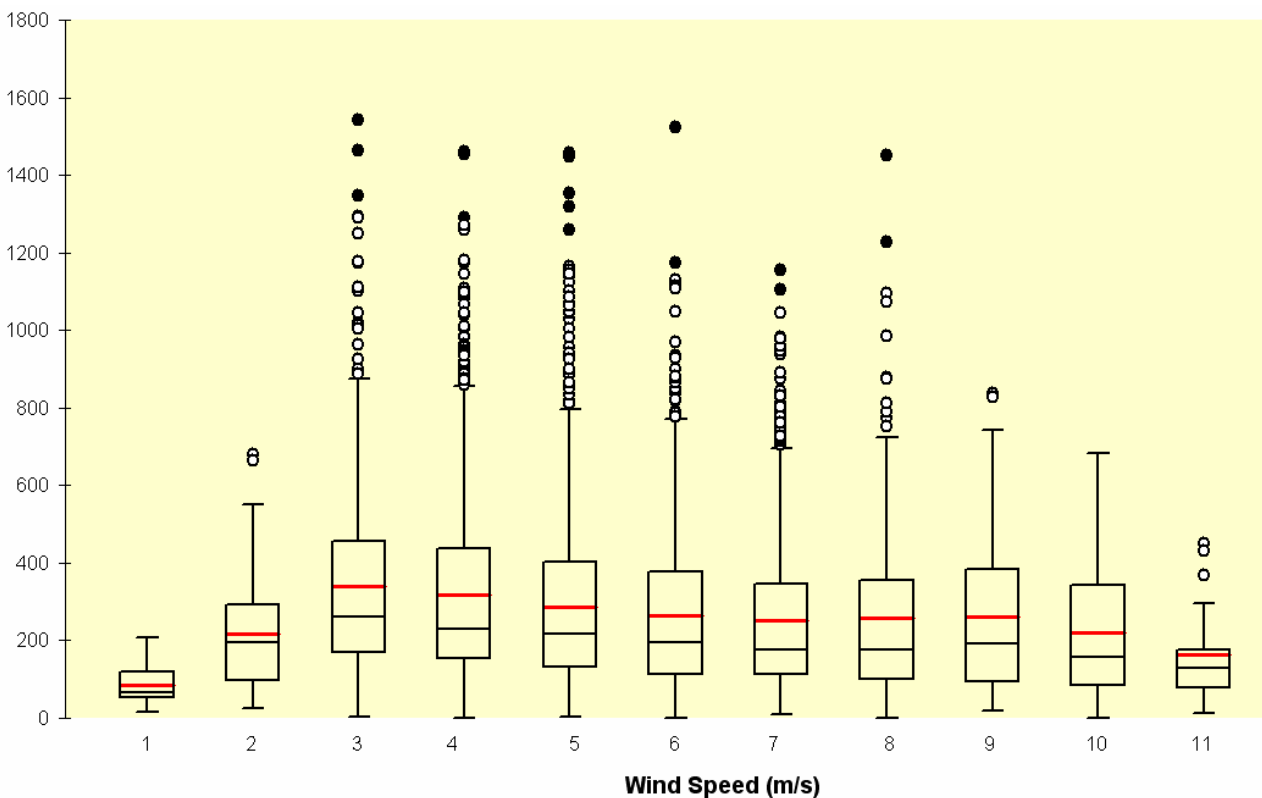


Figure 15 Wind Speed Dependence of NO_x Peak Height (mg/m³). The red lines are the means. The box includes 50% of the values.

3.15 Figure 16 shows the relationship split by aircraft wake vortex category (Heavy and Medium). The shape of the relationship in both cases is very similar over the 3-7 m/s range. It is though of note that the proportional reduction with increasing speed is greater for Medium aircraft than Heavy

aircraft, with a roughly 35% reduction for Medium aircraft over this range and 20% for Heavy aircraft. This suggests there may be some differences in the dispersion characteristics according to aircraft size.

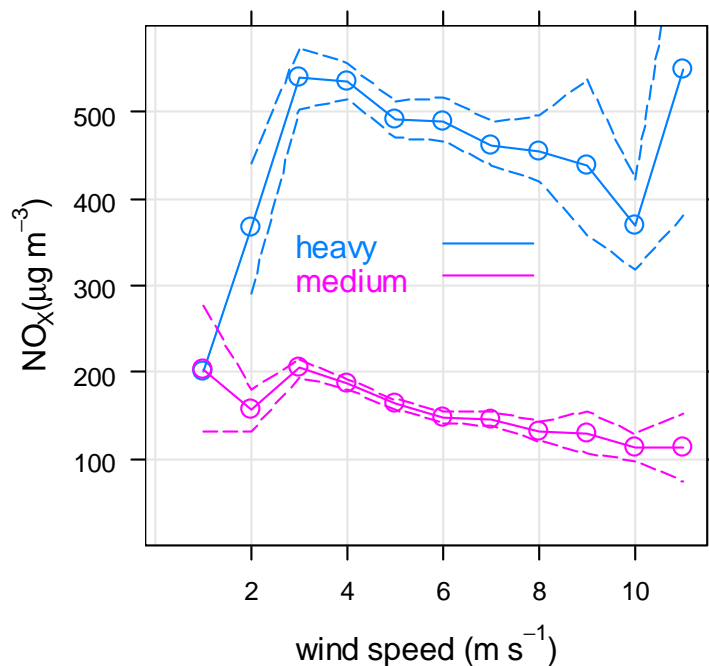


Figure 16 Wind Speed Dependence of NO_x Peak Height by Aircraft Category. Dashed lines show the 95% confidence intervals.

- 3.16 The more variable behaviour of peak height at both extremes of the wind speed range may be due to the smaller number of data points, and hence wider confidence interval. There is though an indication that peak heights are smaller at the lower wind speeds of 1-2 m/s, especially for Heavy aircraft. This may be indicative of increased buoyancy for larger aircraft at low wind speeds compared with smaller aircraft. Furthermore, most of the light wind speed conditions were during winds from the south-east, which would tend to correspond to aircraft at the start of their take-off roll, where buoyancy effects may be especially important. Further comparisons with model predictions would help confirm the likely dispersion characteristics leading to these wind speed relationships.
- 3.17 The wind speed dependence of background and 'other airport' concentrations has also been examined (Figure 17). The background contribution (at LHR8, Oaks Road) shows a typical wind speed dependence of a decreasing concentration with increasing wind speed. For the baseline contribution, which includes both background and other airport sources, there is a more gradual decrease in concentration with wind speed. The difference between these two quantities (baseline – background) should reflect the wind speed dependence of the 'other airport' sources. The pattern

for the 'other airport' sources shares some of the characteristics of the peak dependency on wind speed, i.e. those of an elevated source. This may suggest that the 'other airport' sources are not dominated by low-level sources such as from vehicle emissions, but by sources with buoyancy such as aircraft engines and APUs. Note also that the concentration of NO_x for these 'other airport' sources (baseline-background) increases to a maximum at 5 m/s compared with 3 m/s for aircraft peaks. This behaviour is that expected from a source released at an effective height which is higher than that for the aircraft plumes and may be suggestive of emissions from APUs and taxiing aircraft having a greater buoyancy than aircraft emissions during take-off. No explanation for the dip at 3 m/s has been identified.

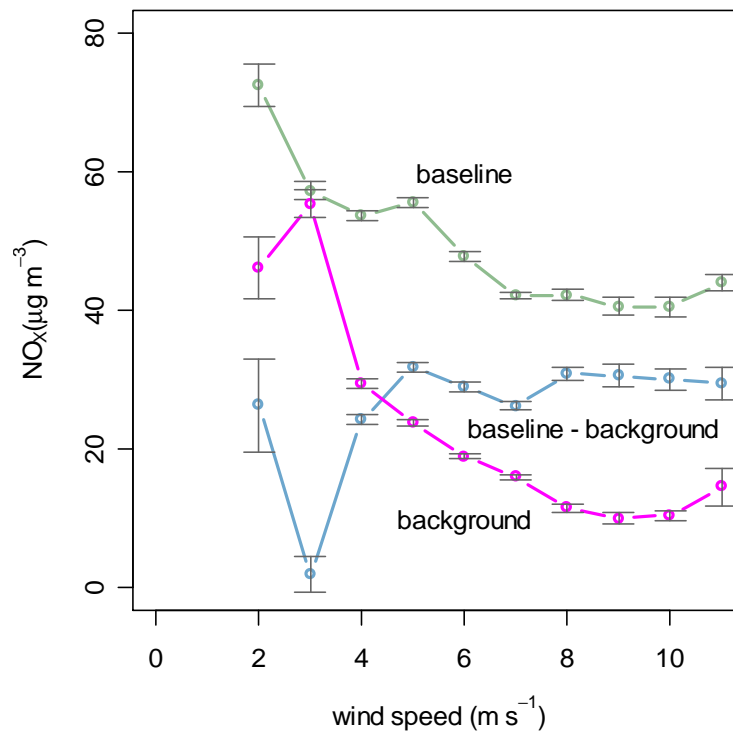


Figure 17 Wind Speed Dependence of Background, Baseline and 'Other Airport' (Baseline – Background) NO_x concentrations. The analysis is based on the 20 days with winds blowing from the airport to LHR2. The values shown are the means and 95th percentile limits.

Role of Atmospheric Stability

- 3.18 Consideration has also been given to the effect of atmospheric stability which is defined by the parameter h/L_{MO} , with negative values indicating unstable atmospheric conditions and positive values more stable conditions. The plot in Figure 12 shows that peak height is not strongly

dependent on atmospheric stability, although there is some evidence of higher peaks with more stable conditions. Figure 18 shows a similar pattern occurs for both Heavy and Medium aircraft types. The tendency for lower peaks to be associated with more unstable conditions may reflect the relationship between stability and wind speed and the peak height dependency on wind speed. It should though be noted that peaks associated with elevated releases tend to be higher under unstable conditions, which bring the plume down to the ground closer to the source.

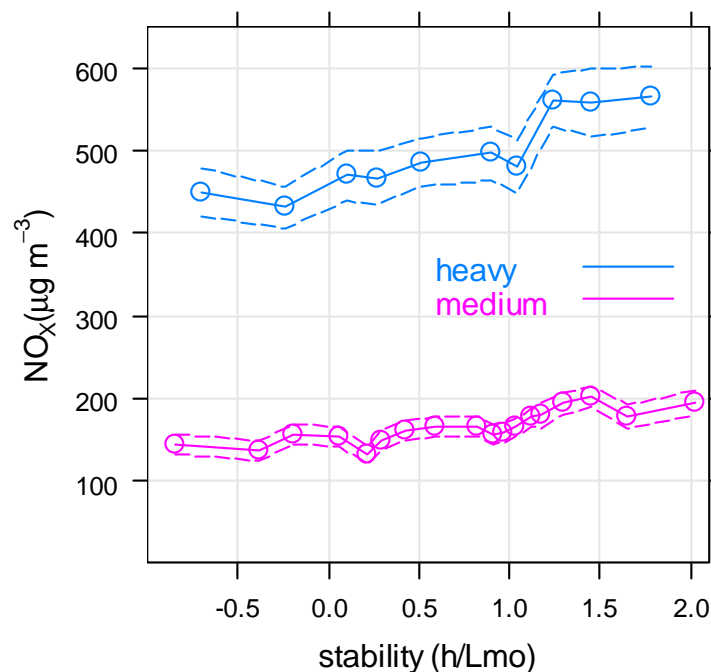


Figure 18 Dependence of NO_x Peak Height on Atmospheric Stability by Aircraft Wake Vortex Category. The dashed lines show the 95th percentile confidence intervals.

Role of Aircraft Type

- 3.19 The mean peak heights have been calculated for each aircraft type, and where sufficient data were available, by airline. To ensure reasonable sample sizes and uncertainty intervals that were not too wide, the data were screened to ensure only groups of more than 30 peaks were analysed. The results of the analysis are shown in Table 2 and in Figure 19.

Table 2 Mean NO_x Peak Height by Aircraft Type (and Airline) and NO_x (take off) Emissions.

Aircraft (Airline)	Mean contribution to NO _x peak (mg/m ³) ^a	Weighted ICAO NO _x emission (g/s)
Boeing 737-other	125 ± 4	43
McDonald Douglas DC9-82	128 ± 18	49
Airbus A319	133 ± 4	41
Airbus A320	161 ± 4	53
Boeing 737-800	185 ± 19	63
Airbus A321	199 ± 6	101
Boeing 757-200	261 ± 14	91
Boeing 767-300 (Air Canada)	329 ± 33	157
Airbus A330-200	374 ± 31	222
Boeing 747-400 (Virgin Atlantic)	375 ± 42	251
Airbus A340-300	380 ± 21	194
Boeing 767-300 (All)	417 ± 24	259
Boeing 777 (American Airlines)	442 ± 25	357
Boeing 747-400 (Air India)	468 ± 48	286
Boeing 767-300 (British Airways)	478 ± 32	359
Airbus A340-600	501 ± 45	402
Boeing 777-200	517 ± 18	358
Boeing 777 (British Airways)	520 ± 24	333
Boeing 777 (United Airlines)	561 ± 53	402
Boeing 777-300	565 ± 82	357
Boeing 747-400 (All)	566 ± 18	430
Boeing 747-400 (British Airways)	606 ± 32	516
Boeing 747-400 (Qantas)	634 ± 48	609

^a 95% confidence interval.

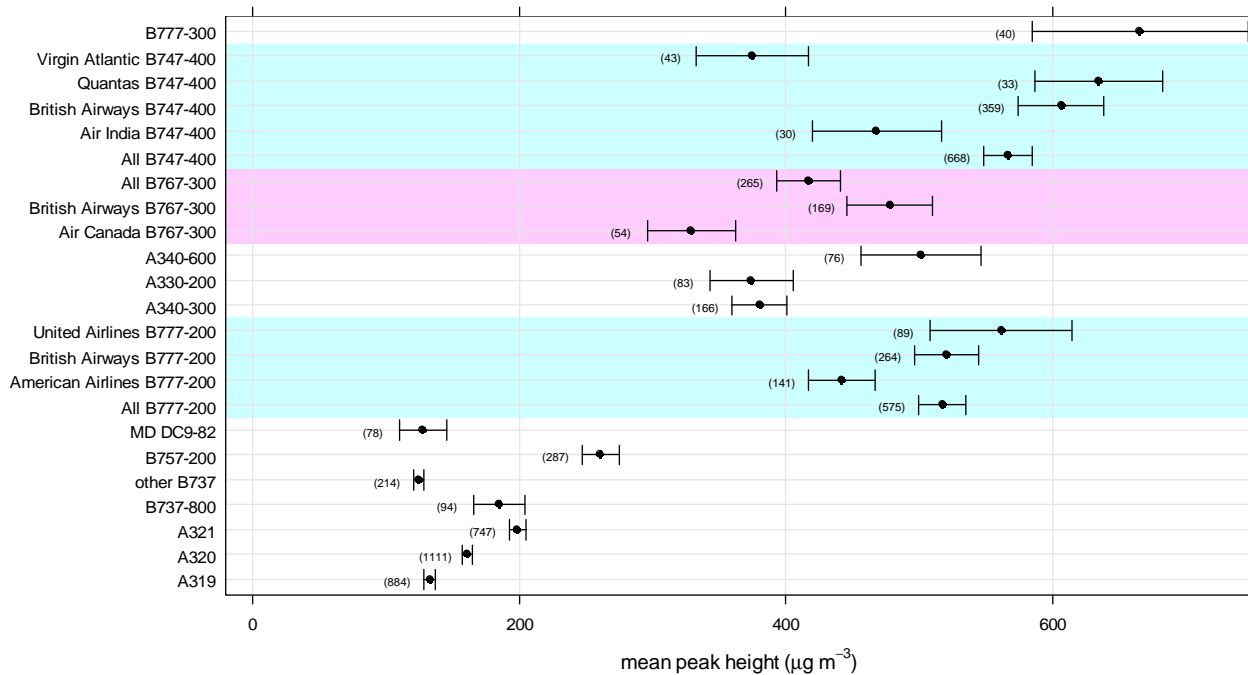


Figure 19 Mean Peak Height for Major Classes of Aircraft and Airline. The uncertainty intervals show the 95% confidence intervals. The shaded areas are regions where it has been possible to disaggregate the aircraft type by airline. Numbers in brackets show the total number of plumes sampled. A minimum of 30 values required for inclusion in the analysis.

3.20 Also shown in Table 2 are the NOx emissions during take-off, obtained from the ICAO database, which presents information by manufacturer and engine type, the latter identified by a unique UID code. Aircraft movement data for Heathrow have been obtained from the emission inventory work carried out by AEA Energy and Environment on behalf of BAA. This includes information on aircraft movements by airline and specific information on engine types used for these aircraft at Heathrow through the UID number (Brian Underwood, personal communication, AEA Energy and Environment). These two data sets have been matched using the UID number to provide information on engine types by airline. It should be noted that the NATS data only provide information by generic aircraft type e.g. Boeing 777-200 and do not describe the many variants of airframe and engine type. Therefore, the analysis has derived generic emission factors by aircraft type, weighted by engine type and total movements, as illustrated in Table 3 for Boeing 777-200 aircraft. It should also be noted that for the purposes of the analyses set out here, the NOx take-off emission rates at 100% thrust have been used. In practice, few aircraft take-off at 100% thrust, a value of 85% being more typical at Heathrow Airport. The pattern of emissions would be similar had the lower thrust values been used, but the absolute emission rates in grammes per second would be lower.

Table 3 Take-off emission characteristics of Boeing 777-200 aircraft at Heathrow.

Aircraft Features			Movements	NO _x Emissions (g/kg-fuel)	Fuel Flow (kg/s)	NO _x Emissions (g/s/engine)
Airline	Aircraft Type	Engine				
BA	772	Trent 895	915	47.8	4.0	193
BA	772	GE90-76B	1968	40.4	2.8	112
BA	772	GE90-90B	623	52.5	3.3	176
BA	77A	GE90-85B	4040	47.3	3.1	147
BA	77A	Trent 895	4324	47.8	4.0	193
BA	77A	GE90-90B	3754	52.5	3.3	176
			Weighted Emission per Aircraft = 332 g/s			
AA	772	Trent 892	641	45.7	3.9	179
AA	77A	Trent 892	7201	45.7	3.9	179
			Weighted Emission per Aircraft = 357 g/s			
UA	772	PW4090	66	61.0	3.9	238
UA	772	PW4084	2919	45.0	3.4	154
UA	77A	PW4090	3712	61.0	3.9	238
			Weighted Emission per Aircraft = 402 g/s			

* BA = British Airways, AA = American Airlines, UA = United Airlines

3.21 Figure 20 shows the comparison between mean peak height for different aircraft and mean take-off emission rates. In general, there is an excellent agreement between the two, but the relationship is non-linear. Taking a log function of emissions gives a straight line relationship shown in Figure 21, with an r^2 value of 0.97.

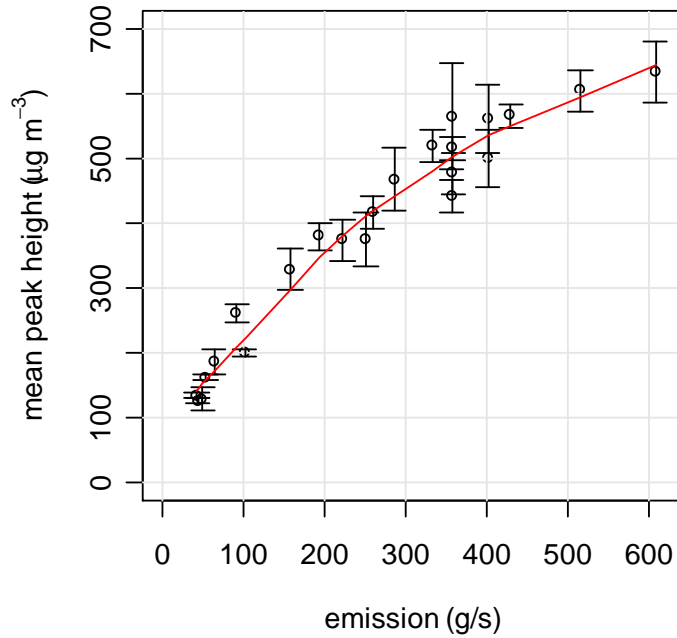


Figure 20 Mean NO_x Peak Height at LHR2 Versus ICAO Take-Off NO_x Emissions. Peak height during take-off on 027R. Take-off emissions at 100% thrust. Thrust varies from aircraft to aircraft and is more typically 85%.

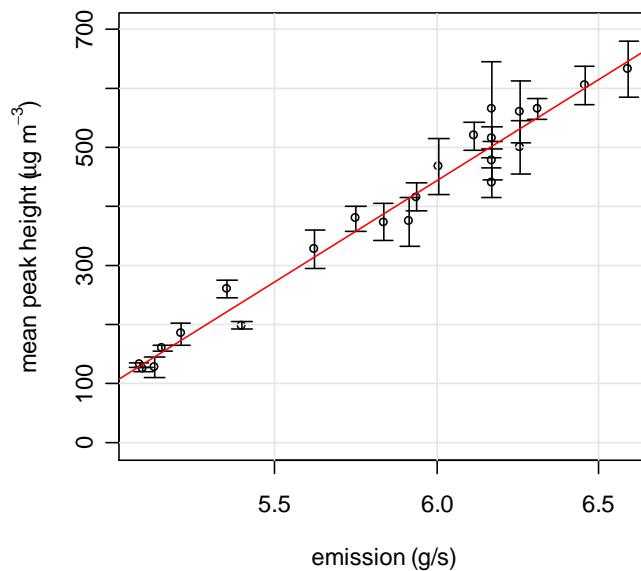


Figure 21 Mean NO_x Peak Height at LHR2 Versus Log of ICAO Take-Off NO_x Emissions. Peak height during take-off on 027R. Take-off emissions at 100% thrust. Thrust varies from aircraft to aircraft and is more typically 85%.

- 3.22 The reasons for the non-linear relationship have not been fully established yet. There are however two factors that could be important. First, the effects of plume buoyancy might be expected to result in a non-linear relationship between emissions and concentrations. This is because the larger aircraft will have higher heat emissions and thus potentially greater buoyancy, which would be expected to give rise to greater plume heights, and lower concentrations detected at the ground level LHR2 monitoring site. Therefore, as aircraft size increases, the detected concentration at LHR2 will not increase in direct proportion to the total emissions of NO_x. The actual behaviour of plume buoyancy for aircraft emissions is currently not well established and thus it is difficult to know what sort of form the relationship might take. Second, it is also possible that the initial dispersion of the plume is greater from the larger aircraft, due to a) a generally wider spacing of the engines, b) a greater volume of air being pushed through the engines, and c) when moving, a larger wake vortex.

Annual Contribution of Aircraft Departing on Runway 027R

- 3.23 This section considers the contribution made by aircraft and other sources at LHR2 using the fast response NO_x data. For the purpose of this analysis, only days for which there are clear peaks are considered, corresponding to the 20 days identified in Appendix E. This subset was considered because the peak extraction is more likely to work reliably when there are clear peaks. These days should also provide a robust estimate of the baseline contribution, i.e. the other on-airport emissions, together with a background contribution assumed to be the NO_x concentration at LHR8 (Oaks Rd).
- 3.24 The results of the source apportionment are shown in Table 4. The aircraft take-off contribution for 027R departures averages approximately six times that for departures on 027L. This indicates that there is roughly a factor of six greater dilution of emissions between a source 180 m and one 1600 m from the monitor. This could usefully be compared with the difference predicted by modelling, as an aid to verifying the performance of the models. The baseline and background contributions are very similar in each case and hence the 'other airport' sources contribution is also very similar. This may also suggest that the peak extraction method works as well for southern runway take-offs, even though the peaks at LHR2 are less distinct². Assuming equal numbers of 027R and 027L runway departures, it can be shown that the 'other airport' sources contribute approximately 20% of total on-airport sources to the concentrations at LHR2. Note that this figure depends on the appropriateness of the LHR8 (Oaks Rd) background site as representing mean concentrations of NO_x entering the airport boundary to the south, although given the location of the LHR8 (Oaks Rd) site and the mean concentration of 26.6 µg/m³, this contribution seems reasonable.

² The peaks matching for take-offs on the southern runway 027L were only derived using the automated technique.

Table 4 Source Apportionment of NO_x Concentrations at LHR2 (mg/m³).

Source	Contribution During 027R Take-Off	Contribution During 027L Take-Off
Aircraft Departures	154	27
Baseline Contribution	50	49
Background (LHR8, Oaks Rd)	26	27
Other Airport Sources (Baseline-Background)	24	22
Total	204	76

3.25 The mean peak heights calculated by aircraft type can be used to estimate the long-term average contribution made by aircraft departing on runway 027R to NO_x concentrations at LHR2, weighted by aircraft movements. Using NATS data from 2003 and 2004, mean peak heights have been ascribed to 87% of all aircraft movements. Table 5 shows the contribution made by aircraft type, and shows for example that Boeing 747-400s account for about 25% of the total NO_x concentration contributed by aircraft at LHR2. Note that these data are based on departures from 027R.

Table 5 Contribution of Aircraft to NO_x Peaks at LHR2 for Take-offs on Runway 027R.

Aircraft	Contribution (%)
B744	25.3
B772	17.1
A320	14.3
B763	9.6
A321	9.2
A319	7.8
B752	5.3
A343	3.7
A332	1.8
B734	1.2
A346	1.2
B773	1.1
B738	1.0
MD82	0.8
B735	0.5
B736	0.2

- 3.26 The contribution of aircraft departing on 027R to the annual mean concentration at LHR2 has been estimated from the 15-minute average concentrations. To do this, the 15-minute average baseline concentration, as defined in para 2.9, has been subtracted from the total 15-minute concentration for the periods with take-offs on 027R on the 20 days identified in Appendix E. These 15-minute concentrations have been grouped by wind sector³ and the averages are shown in Figure 22. These average contributions have been applied to the full wind data set for 2005 at LHR2, assuming operation of runway 027R during the period 06:30 to 15:00 h or the period 15:00 to 23:30 hours, with take-offs for winds between 140-180° restricted to wind speeds 3m/s or less. All other winds were assigned a zero contribution.
- 3.27 The average NO_x concentration during 2005 at LHR2, due to take-offs on runway 027R derived in this way is 25.6 µg/m³ assuming all take-offs are during the morning period and 25.9 µg/m³ for the afternoon period, giving an overall average of 25.7 µg/m³. The total contribution from the airport would be somewhat higher than this due to the 'other airport' sources and take-offs on the southern runway. A simple scaling from the source apportionment in Table 4 would suggest that an additional 30% would come from other airport sources⁴ and 17.5% from aircraft departing on the southern runway, which would indicate an additional contribution from these sources of 47.5% of the value for aircraft departing on 027R, or 12.2 µg/m³, to give a total airport contribution to the annual mean NO_x concentration at LHR2 of 37.9 µg/m³. This total airport contribution shows reasonable agreement with the estimate, of 31.5 µg/m³ during 2002, made using a different approach in the PSDH report (DfT, 2006)⁵.

³ 140-160°, then 10° sectors up to 280° and finally the 280-310° sector.

⁴ The other airport sources contribute 15% (23/154) during take-offs on the northern runway, which doubles to 30% for a full day.

⁵ This is the contribution from sources within the airport boundary. It does not include NO_x from airport-related traffic in the locality.

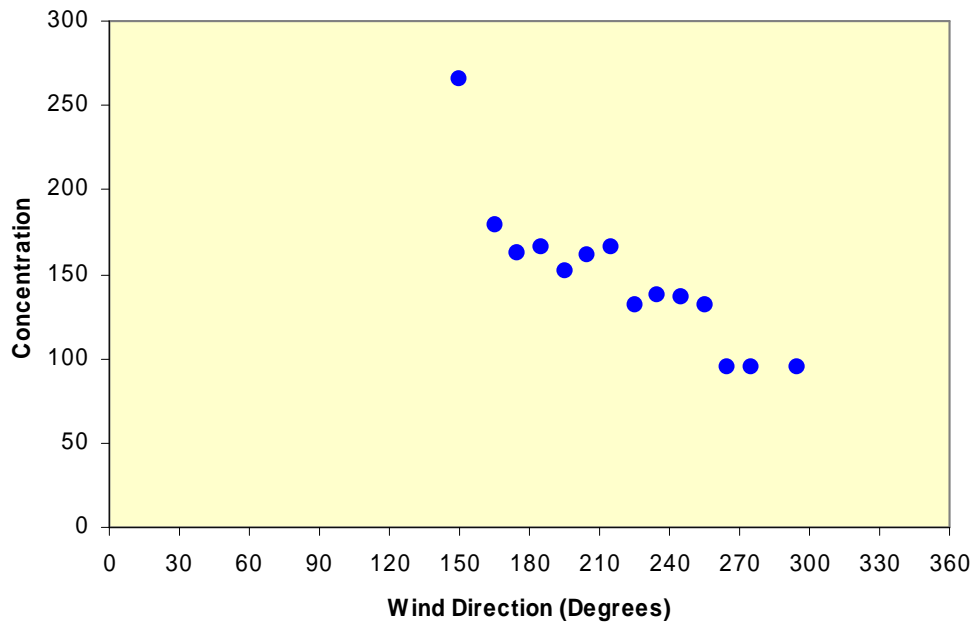


Figure 22 Average Contribution of Aircraft Departing on Runway 027R to 15-minute Concentrations (mg/m³) at LHR2 for Different Wind Directions. For the period when departures are taking place.

4 Conclusions and Recommendations

4.1 The PSDH report identified the requirement for further assessments of air quality at Heathrow in order to improve the emissions inventory data and to enhance the selected model approaches. The work carried out in this study provides an important analysis of aircraft emission contributions that can be used to assist with improving the parameterization of the initial plume dispersion, and with more extensive model verification tests

4.2 The data collected and analysis contained in this report represent a unique data set of multiple plume sampling from individual aircraft at Heathrow Airport. This work has highlighted the following:

- It has been shown that methods can be developed to analyse and characterise thousands of individual plume samples from individual aircraft. Chromatographic techniques have proved to be an effective approach to extract various peak characteristics and identify for example, the contribution made solely by aircraft take-off emissions.
- The two methods developed to match plume NO_x measurements with aircraft movements demonstrate that the matching process is robust and reliable.
- Clear differences in the mean height of peaks can be delineated for different aircraft (and airline) types. Furthermore, robust uncertainty intervals can be calculated using appropriate statistics.
- No difference in peak shape could be detected between four and two-engined aircraft. The mean peak shape for each aircraft type is approximately Gaussian and only showed slight asymmetry.
- Comparisons between measured NO_x plume peak heights and mean aircraft fleet emissions have been made using data from the ICAO emissions database.
- There is a non-linear relationship between the mean peak height and the ICAO emissions, such that larger aircraft with higher-emitting NO_x engines result in proportionately less measured ambient NO_x. Currently, the origins of the non-linear relationship are not fully understood, but a plausible explanation is that larger aircraft engines are associated with higher total heat emissions and therefore increased plume buoyancy. As a consequence, the ground-level concentrations of NO_x from larger aircraft are proportionately less than smaller-engined aircraft.

- A log-offset transform of the emissions data results in a convincingly linear relationship between mean airline ICAO emissions and mean peak height ($r^2 = 0.97$). This finding may help determine the origin of the non-linear relationship e.g. by helping to determine the type of parameterisation necessary for buoyancy to explain the relationship.

4.3 The following recommendations arise out of this work:

- The data set collected is very likely to yield further important findings if further analysis is carried out. In particular, a comparison with models such as ADMS-Airport would be very useful and could yield useful information on model performance and deficiencies.
- The current study has been limited by the availability of aggregated engine-type data by airline. If engine data and aircraft operational information (such as thrust setting) were available on for individual aircraft, it is very likely that considerably more insight could be gained.
- Consideration should be given to a further measurement campaign and the measurement of CO₂. Simultaneous measurements of CO₂ and NO_x would allow for a direct and robust comparison with the ICAO database. Furthermore, the logging of individual aircraft engine types and operational characteristics would lead to a much-improved understanding aircraft emissions and dispersion behaviour.
- The results of the analysis should be compared with dispersion modelling outputs. This comparison would help with model validation and provide information concerning some of the important factors affecting near-field plume dispersion from aircraft engines.
- It would be useful to estimate the contribution of aircraft taking-off to annual mean NO_x concentrations at LHR2. This will allow comparisons to be made with previous estimates using different approaches.

References

- Carslaw D.C., Beevers S.D. and M.C. Bell (2006). Modelling and assessing trends in traffic-related emissions in a street canyon location using a generalized additive modelling approach. Atmospheric Environment (in press).
- DfT (2006) Project for the Sustainable Development of Heathrow - Air Quality Technical Report, <http://www.dft.gov.uk/pgr/aviation/environmentalissues/secheatrowsustain/>
- Nielsen N-P.V., Carstensen J.M., Smedsgaard J.A. (1998) On Single and Multiple Wavelength Chromatographic Profiles for Chemometric Data Analysis Using Correlation Optimised Warping, Journal of Chromatography, Vol A (805), 17-35.

Acknowledgements

Thanks are due to:

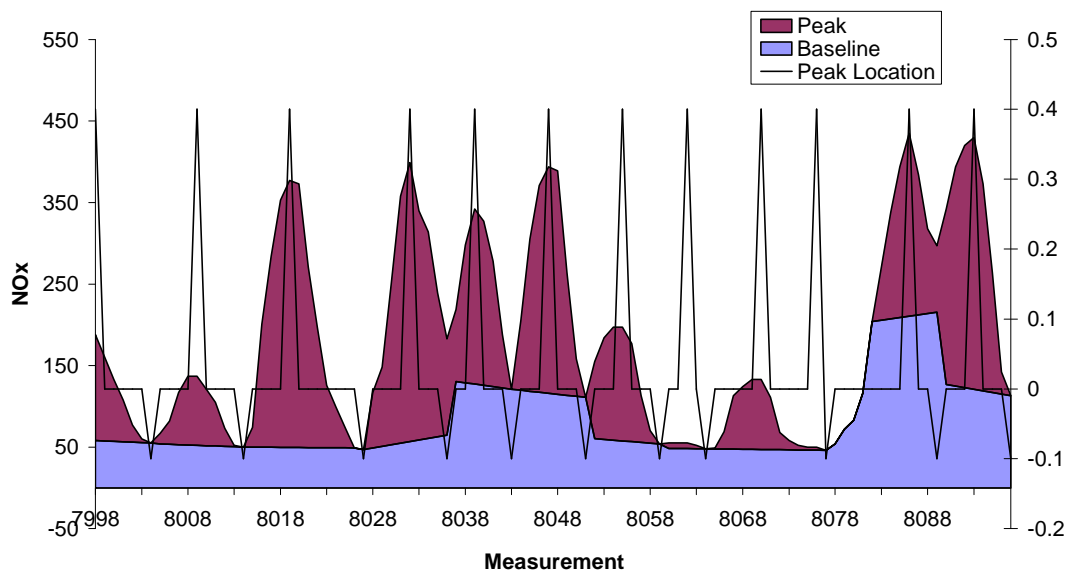
Dr Martin Williams of Defra for his helpful comments

Brian Stacey at AEA Energy and Environment for provision of the NO_x data.

Appendix A - Isolation of Peaks from Baseline

1. The differential (dy/dx) was used as an initial screening parameter to identify 'candidate' peak tops ($dy/dx = 0$; before +ve, after -ve) and peak bottoms ($dy/dx = 0$; before +ve, after -ve). Because this type of approach can be subject to interference from analytical noise, the 'candidates' were further screened using two sets of likelihood rules: the first screened 'candidate' peak tops and bottoms to remove peak 'shoulders' and artefacts, e.g., 'candidates' that were outside the logical sequence – alternating tops and bottoms – each time excluding the lower top or higher bottom as appropriate; while the second set of rules corrected the peak tops and bottoms on 'atypical' peak, e.g. foreshorten highly asymmetrical peaks, applying a common baseline to overlapping peaks, etc.. Two estimations of baseline were then produced: firstly, an initial estimate extrapolated by joining peak bottoms; and secondly, by applying one of three cut-off rules (clustering, common baseline, median) to the initial baseline estimation. These measurements were then used to determine a range of common peak parameters (location, width, area height). Finally, the software screens the results to remove noise (using peak area and height thresholds). All screening/fitting parameters can be set from a graphical interface to simplify the peak integration parameter selection process. Example software outputs are shown in Figure A1.

(A) Initial Peak Assignment



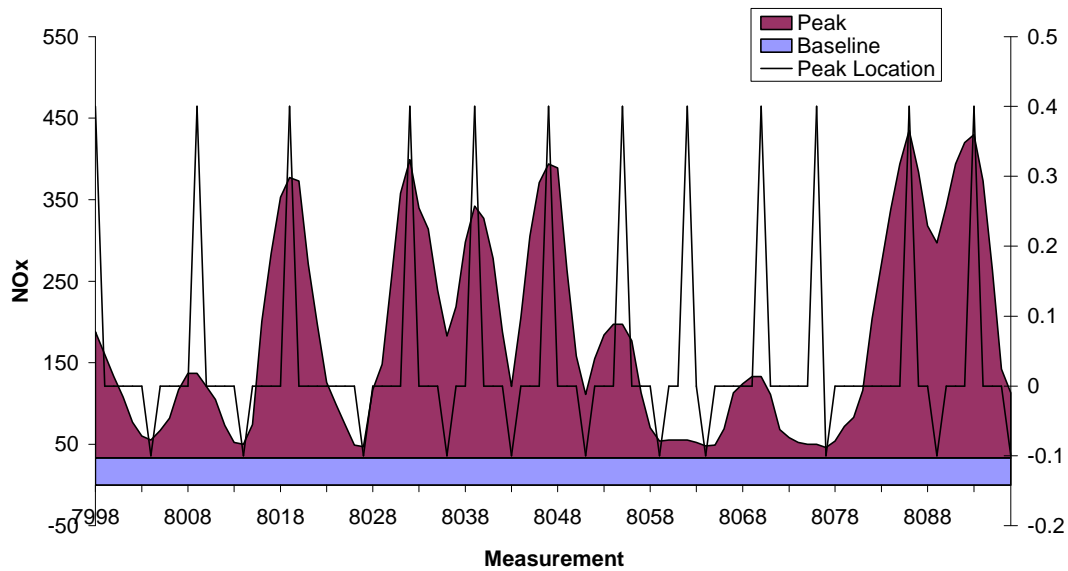
(B) Corrected Peak Assignment

Figure A1: Example of peak location and integration using region 8000-8100 from Figure 1. Identified peak tops and bottoms are indicated by maxima and minima on the arbitrarily scaled (-0.1 to 0.4) marker 'Peak Location'. Sections A and B show integration before and after median baseline realignment using median cut-off.

Appendix B – Semi-Automated Alignment of NO_x Peaks to Aircraft Departures on Runway 027R

2. Stage 1 involved applying the following procedure for each day separately:
 - The times of each Heavy aircraft take-off during the day were plotted on a time series, by assigning a data point based on the concurrent measured NO_x concentration. The measured NO_x concentration time-series was then plotted on the same graph. For the majority of days, it was very clear that the first Heavy take-off from 027R coincided roughly (but not exactly) with the first major peak. The time delay between the first Heavy take-off and the first peak was thus introduced as an offset to the entire daily aircraft movement dataset, so that the first Heavy take-off coincided precisely (within 10 seconds) with the first major concentration peak. Data for each consecutive hour on that day were then examined and the offset was adjusted if necessary in order to retain a relatively close match between the Heavy take-offs and the major peaks throughout the day.
 - During this examination of the data, “other” aircraft movements were also looked at, albeit briefly, and if necessary a separate offset was introduced into this dataset. The primary focus was, however, on the Heavy aircraft since the very large number of “other” movements made even this cursory examination difficult.
 - For a small number of days no clear peaks were apparent and it was not possible to match the two datasets. These were all days associated with winds not blowing from the runway towards the monitoring site.
3. This first stage of data examination only aligned the two time series to within a few tens of seconds of each other. The sheer volume of data precluded a more precise visual matching of the entire dataset. The second stage was thus to more precisely match each concentration peak with its corresponding take-off, as follows:
 - The exact timing of each concentration peak was taken from the analysis described in the section on Isolation of Concentration Peaks from Baseline. Simple spreadsheet algorithms were then written which snapped the timing of each aircraft departure to the timing of the closest peak concentration. This snapping began with a search band of +/- 10 seconds (i.e. aircraft movements were only matched to a peak if the two data points were within 10 seconds of one another following the Stage 1 analysis). The search band was then progressively extended to +/- 20 seconds and +/- 30 seconds. It is considered that the further this searching

extended from the default offset (as defined in Stage 1), the greater the potential for erroneous pairing became. Each pair was thus assigned a reliability category relating to the extent of search banding required (i.e. 10 seconds or less; 20 seconds; or 30 seconds). Finally, each paired dataset was examined to ensure that both time-series proceeded in chronological order and that no duplication had occurred.

Appendix C - Automated Alignment of NO_x Peaks to Aircraft Departures

4. Correlation Optimised Warping (COW) is one of a number of warping techniques most commonly used to align chromatograms of similar mixtures, but also used to align the results of split analysis methods (i.e., where the sample eluting from a chromatograph is split and then separately analysed using different techniques, e.g. mass spectrometry and FTIR). In all cases, the analyst identifies one time series as a target and the software distorts other time series to better match these to the target. In COW the target time series is divided into a number of equal length sections and for each section in turn the best fit is found by warping (compressing or expanding) the associated section of the non-target time series. This process is depicted in Figure C1 which is taken from Nielsen et al (1998), one of a number of papers describing this procedure. COW optimises the warp fit for the whole data range, making it particularly effective for the alignment of time series with discrete ends.

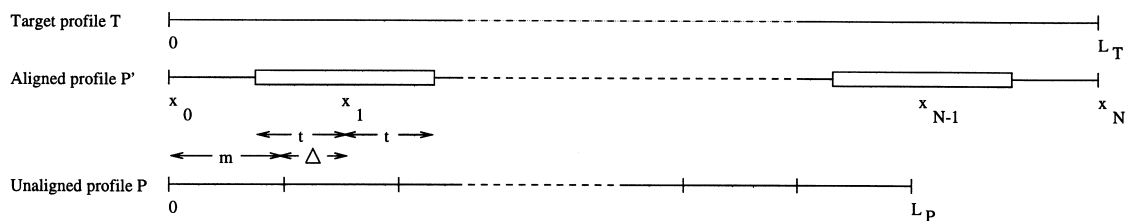


Figure C1 Basic schematic of the COW procedure (source: Nielsen et al, 1998). T is the target profile (e.g. a chromatogram or time series) to which a second profile, P, is fitted. Two user parameters are required, m (the length of sections in T to be fitted) and t (the warping tolerance). An additional tolerance function, Δ , is also used if T and P are different lengths and is equal to the difference between the lengths of T and P divided by m .

5. The diurnal pattern of aircraft activity (i.e., little to no activity in the early hours of the day, high activity during the daytime, little to no activity overnight) provides a usable data set with clear ends. For each day, an aircraft time series was generated at 10-second resolution using a simple set of scoring rules (for each time interval; no aircraft = 0, aircraft 27L = 1, 27R = 10). Therefore, the only applied assumption was that 27R take-offs give rise to larger contributions than 27L take-offs and, importantly, no assumptions were made regarding the relative size of emissions from different aircraft types. The analysis considered the possibility of movements of aircraft on 27L in case they at times made a contribution to the time series of all peaks. These were then fitted to the

associated NO_x peak data series using COW (m =10 measurements or 100 seconds, t = 2 measurements or 20 seconds). Finally, because COW often warped the aircraft time series into or near the range of a given peak rather than to the peak top and 'blurred' some aircraft peaks, a 'clean up' routine was applied that reassigned aircraft data to NO_x peak tops and estimates the reliability of fit (score: 2 = aircraft report matches NO_x peak top, 1 = aircraft report within peak width of NO_x peak and no alternative assignments possible, -1 = aircraft report within peak width of NO_x but alternative assignments possible). In addition, a set of different cases were observed that appeared analogous to 'co-elution of two or more peaks' or 'peak splitting' in chromatographic analysis were also observed and these were scored values < -1. In current applications only peaks with fitting scores ≥ 1 are treated as reliable assignments.

Appendix D – Identification of NO_x Peaks During Take-offs on Runway 027L

1. One important question is whether NO_x concentrations at LHR2 during take-off from 027L (1600 m away) and landing on 027R are dominated by take-off emissions or landing emissions (180 m away). This issue has not been analysed extensively here, but some indication can be gained by considering the diurnal profiles of landing and take-off movements and concentrations. It is difficult to determine these effects from the fast-response data alone because peak matching was only carried out for take-offs on 027R. To help address this question, consideration has been given to hourly data at LHR2 during 2003 and 2004, filtered by runway use and wind direction (160-260 degrees).
2. The diurnal contribution made by take-off and landings is shown in Figure D1. The plot was calculated by weighting the aircraft movements with estimated peak NO_x heights using NATS data for 2003 and 2004. Note that in this case the same weighting has been given to take-off and landing contributions, as the purpose is to emphasise the shape of the diurnal profile. It is also assumed that landing emissions are proportional in some way to the calculated take-off emissions, which might not be the case. The Figure shows that the two profiles are markedly different. For example, there are more large aircraft landing early in the morning compared with the rest of the day and this has the effect of skewing the profile.

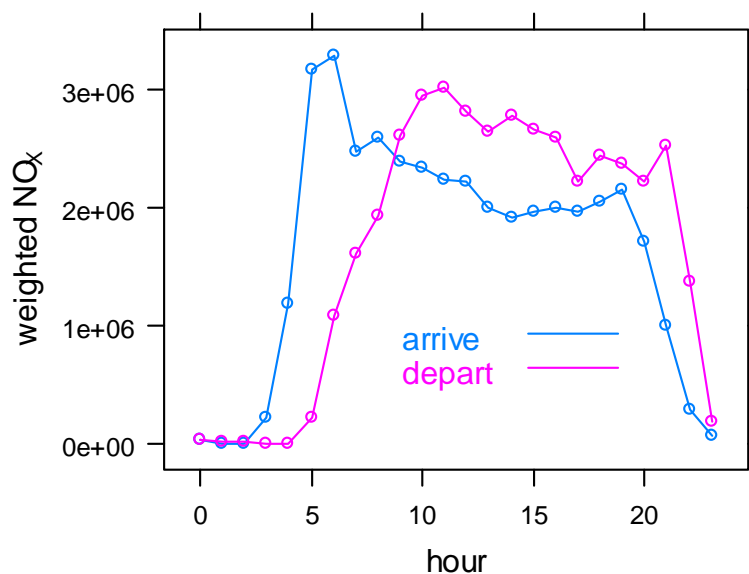


Figure D1 Pattern of Emissions of NO_x during Take-off and Landing.

3. Figure D1 can be compared with the diurnal profile of measured NO_x at LHR2, filtered for 027R take-offs and 027R landings. Both of these profiles are affected by meteorological factors, as shown for example in Figure D2. This plot shows a dip in the middle of the day due to meteorological factors and variation due to the influence of background concentrations.

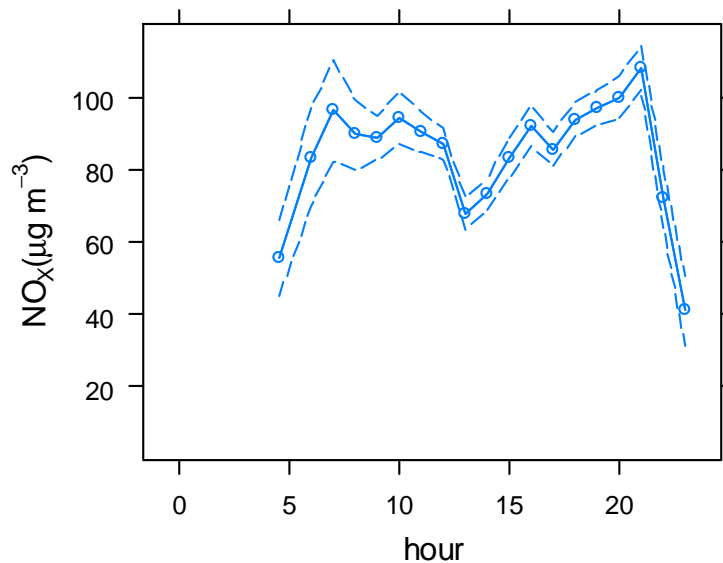


Figure D2 Pattern of NO_x Concentrations at LHR2 by time of day.

4. A better indication of the diurnal profiles can be determined by removing the influence due to meteorological variation. This can be achieved by modelling the hourly concentrations using appropriate covariates. Similar work was carried out by Carslaw et al. (2007). The following model was used:

$$\text{NO}_x = s(u, v) + s(\text{hour}) + s(h/L_{MO}) + s(\text{temp})$$

5. Where NO_x is the hourly measured concentration of NO_x at LHR2, u is defined as [wind speed].sine([wind direction]) and v as [wind speed].cosine([wind direction]); with u positive from the east and v positive from the north, s(hour) is a smooth function of hour of the day (representing the diurnal variation), s(h/L_{MO}) is a smooth function of atmospheric stability and s(temp) is a smooth function of temperature.
6. Figure D3 shows the resulting diurnal profiles, which more clearly follows the variation in aircraft movements weighted by NO_x emissions. Of interest is the 27R landing plot (corresponding to 27L

take-off). This plot shows very little indication of an early morning peak that could be due to large numbers of heavy aircraft landing on 027R. It should be noted however that other airport sources of NO_x are likely to be important for this plot because the estimated contribution of aircraft departing on 027L and other sources of NO_x are similar as shown in Table 4.

7. While these results do not definitively show that it is likely that LHR2 NO_x concentrations are dominated by take-off emissions on 027L rather than landing emissions on 027R, they do provide some evidence that this is likely to be the case. Further work could usefully be carried out to confirm these findings.

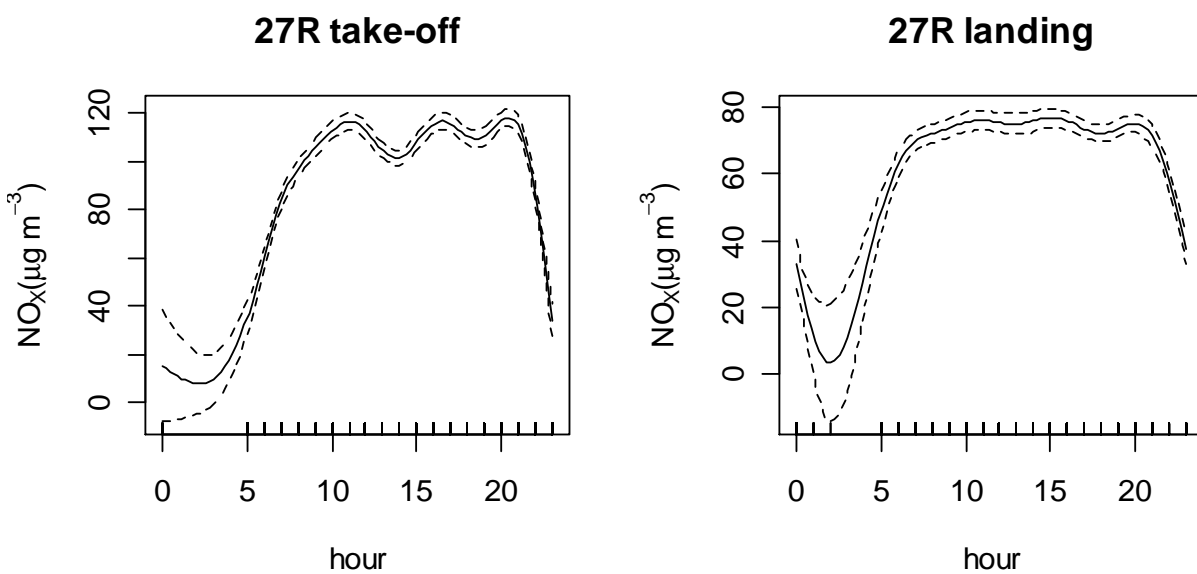
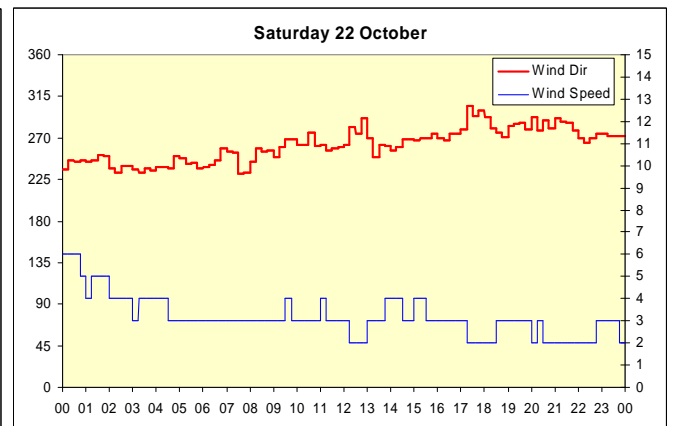
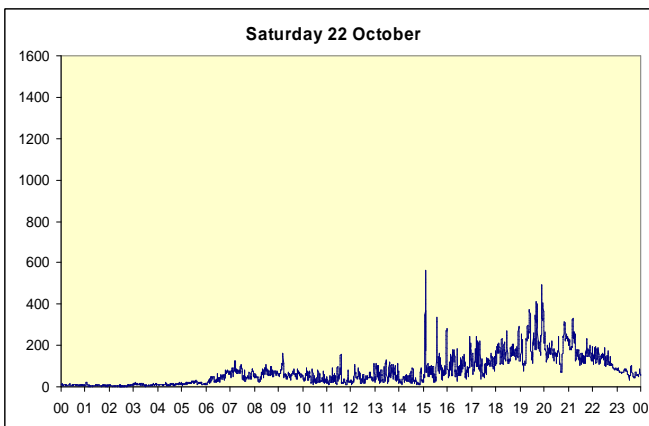
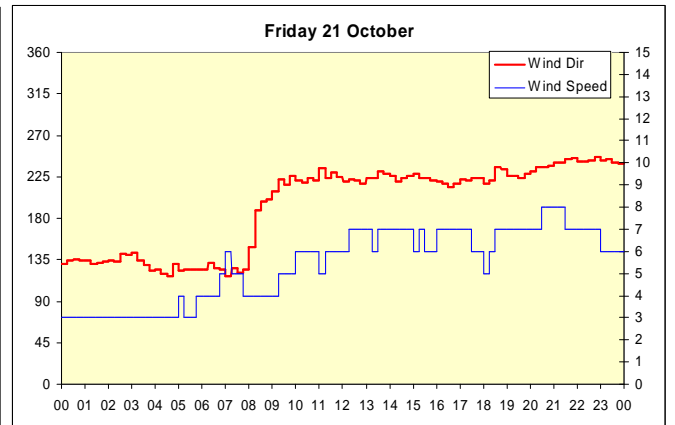
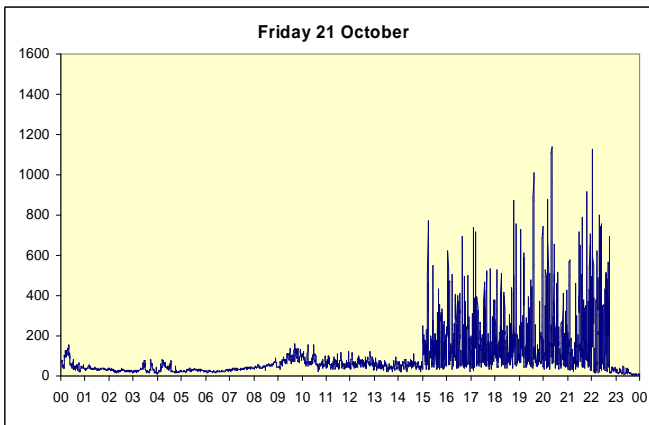
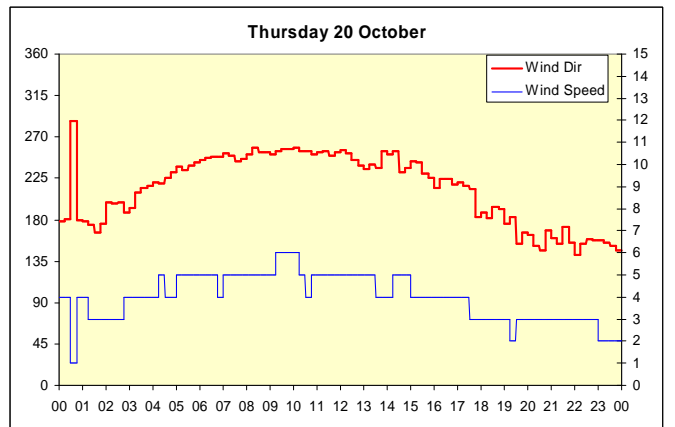
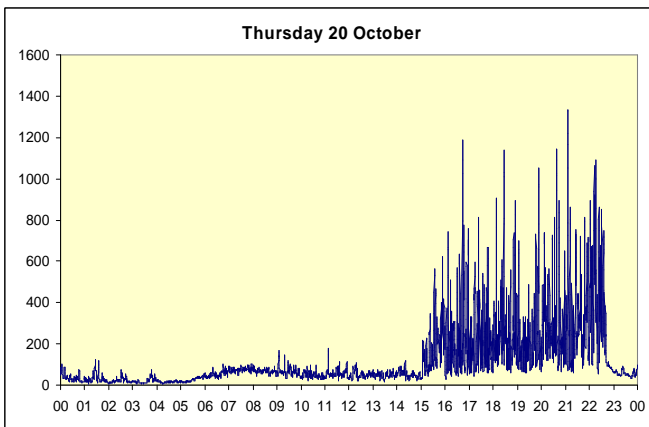
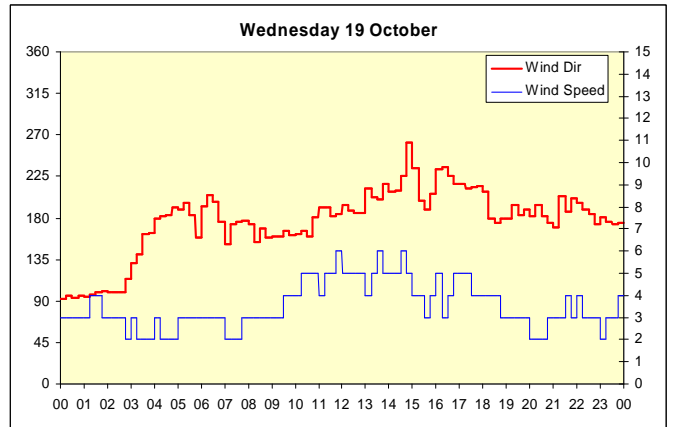
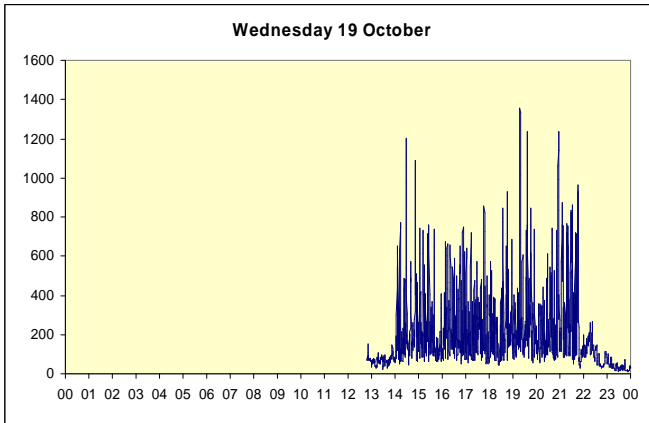
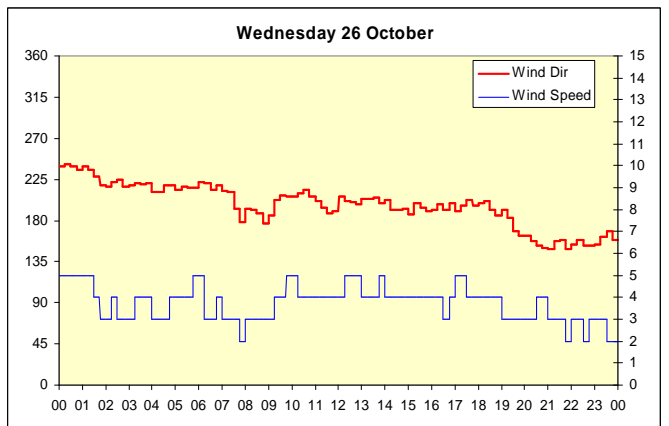
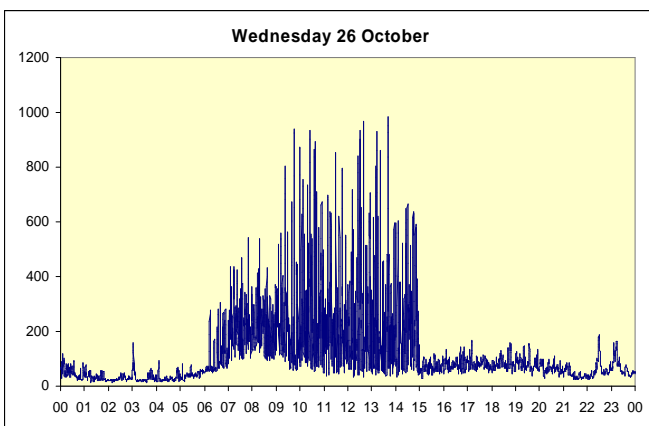
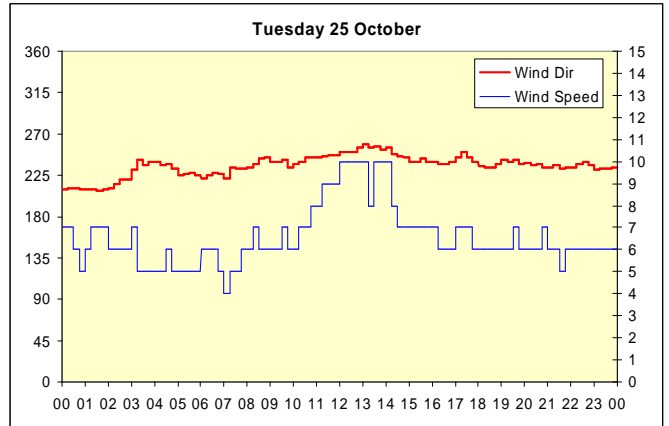
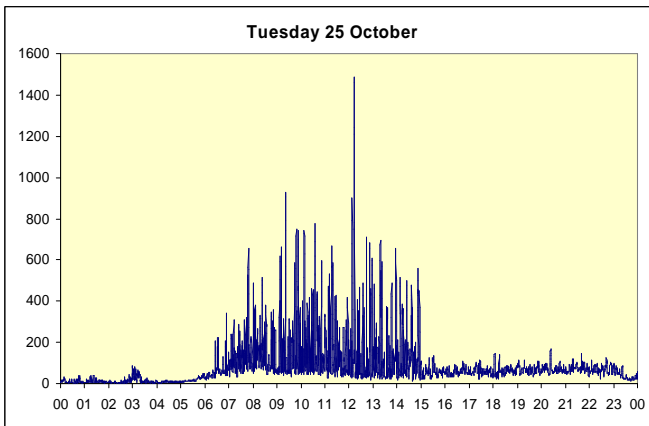
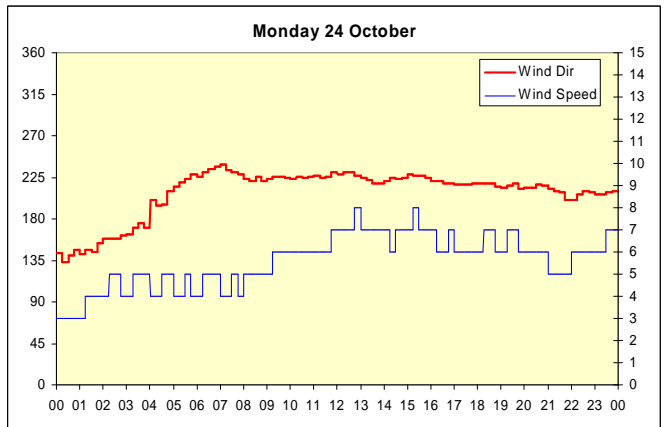
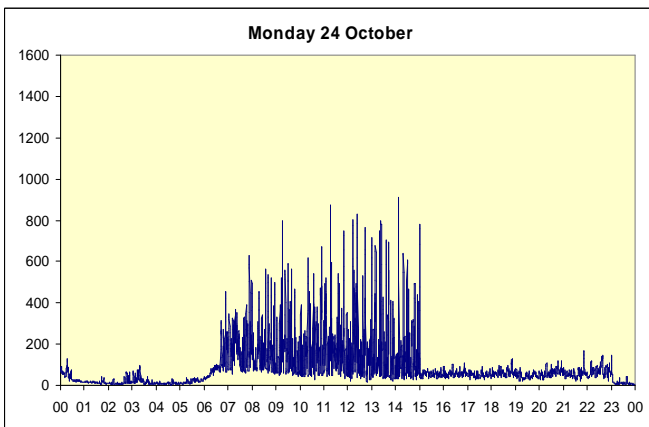
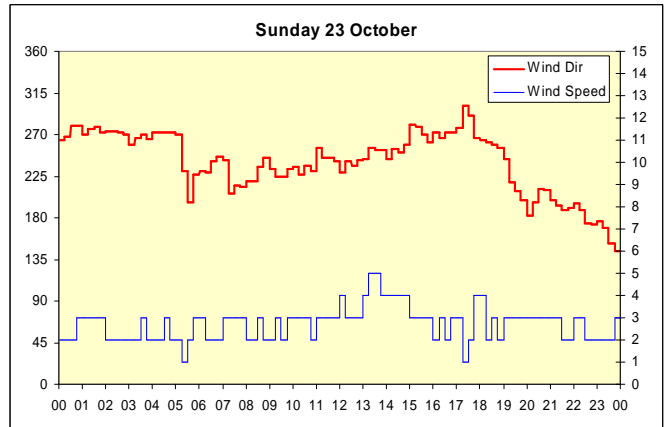
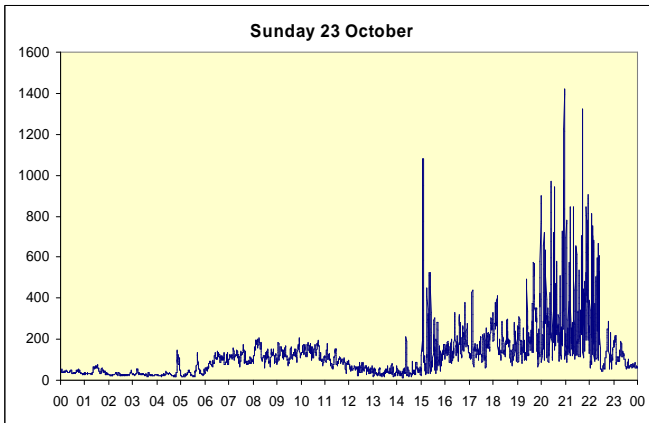


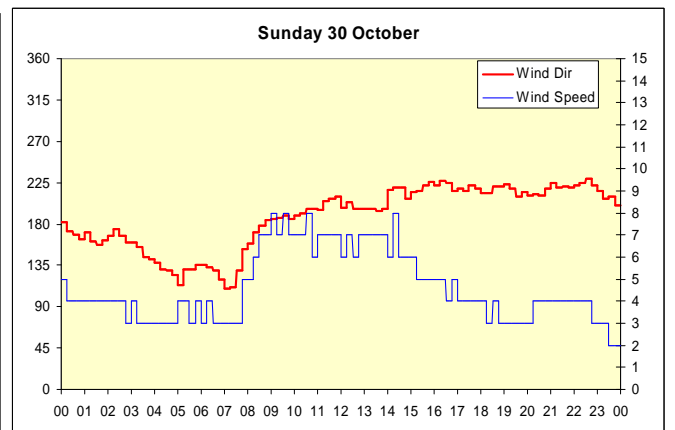
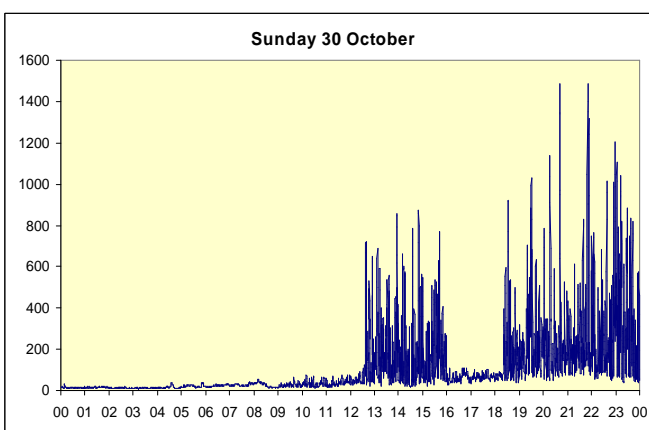
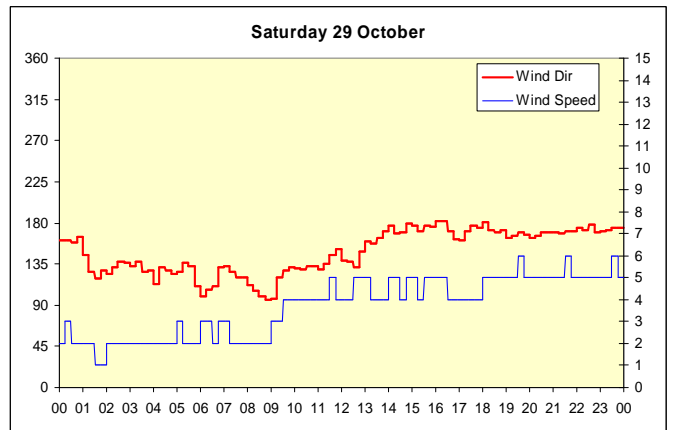
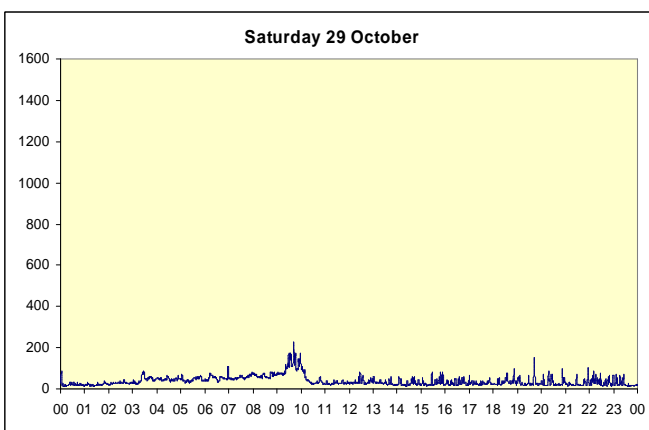
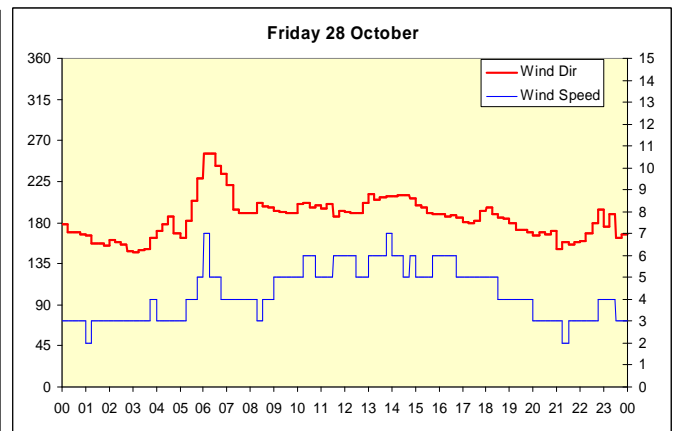
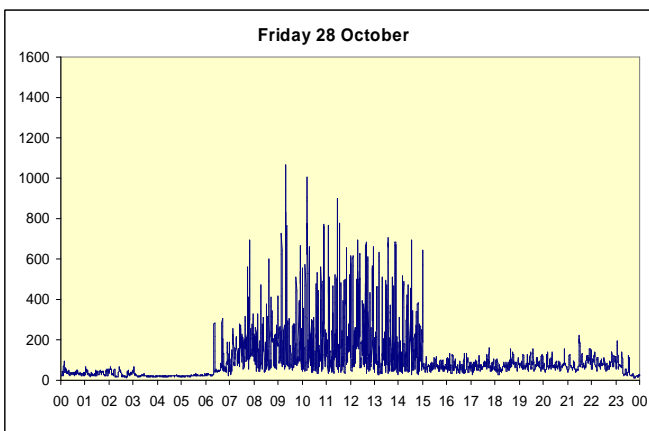
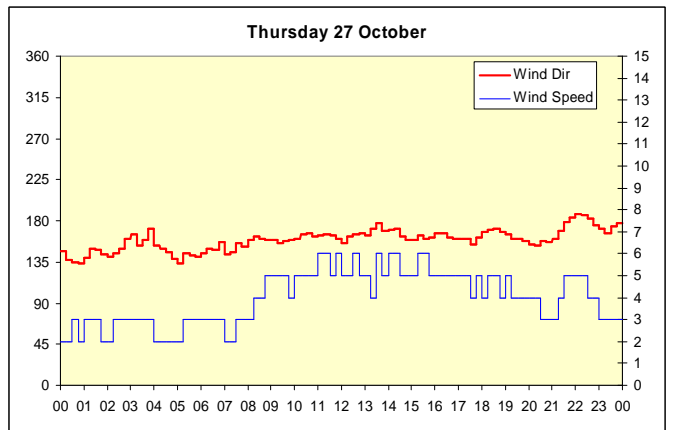
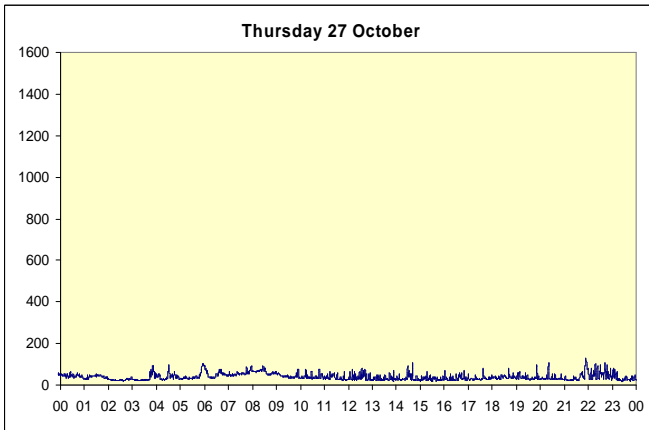
Figure D2 Pattern of NO_x Concentrations at LHR2 by Time of Day, for Aircraft Taking-Off on Runway 027R or Landing on Runway 027R (with Take-Offs on 027L).

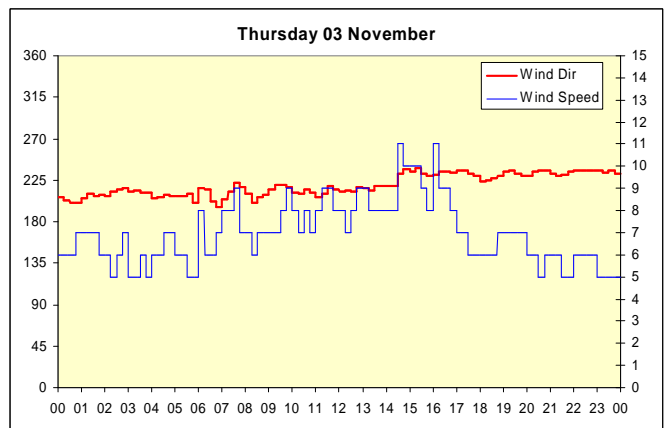
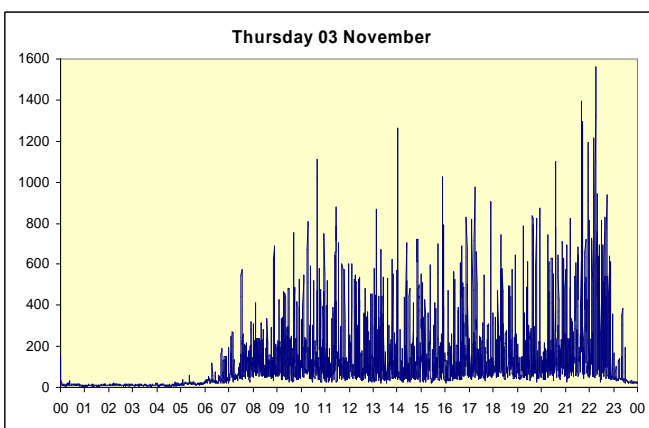
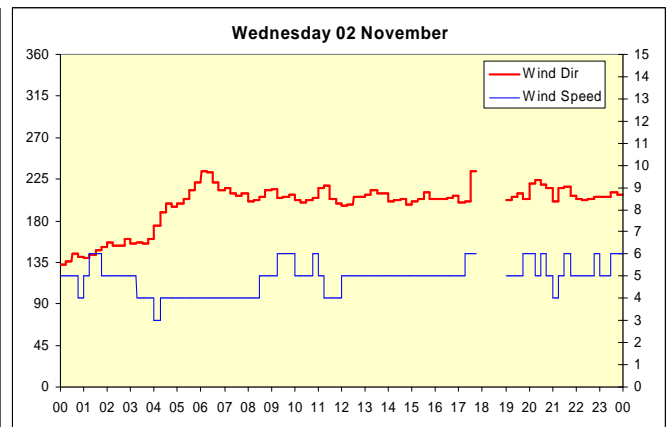
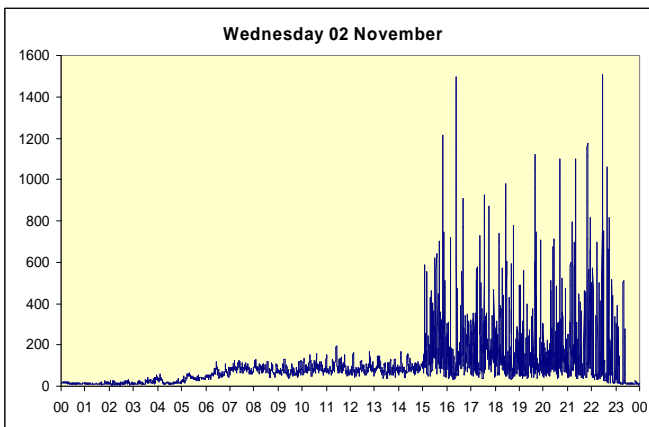
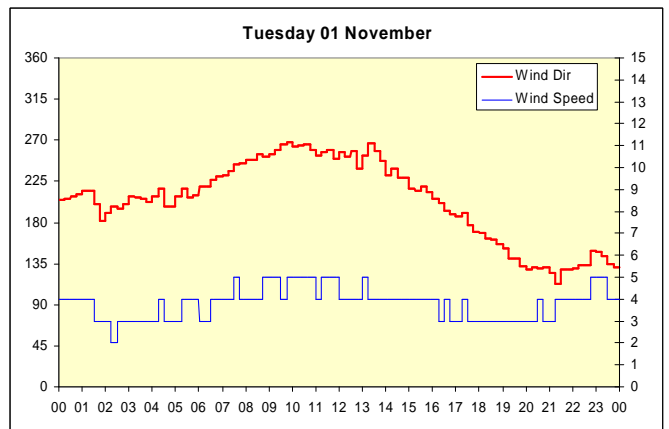
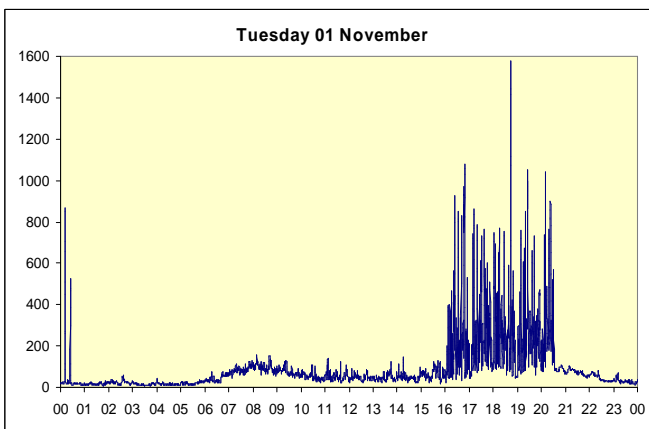
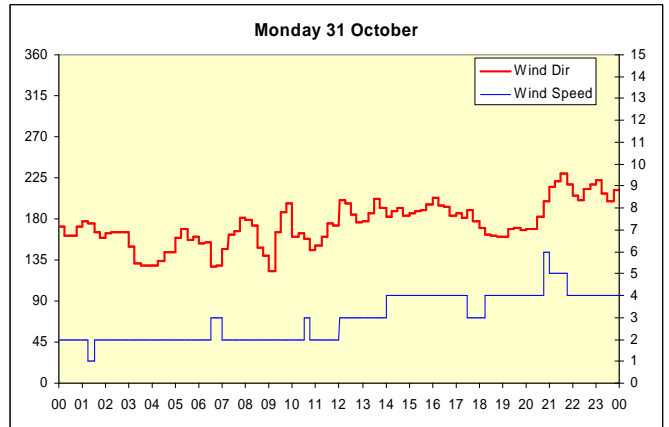
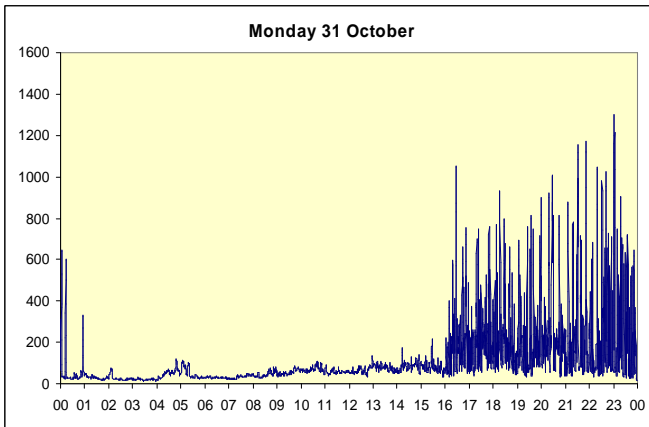
Appendix E – Daily Plots of 10-second NO_x Concentrations and 15-minute Wind Speed and Wind Directions at LHR2

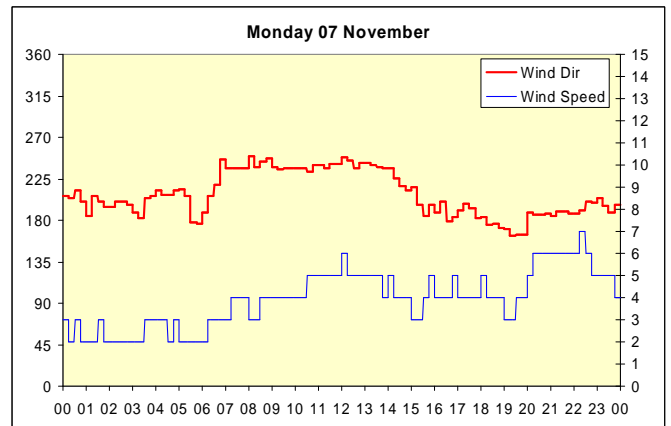
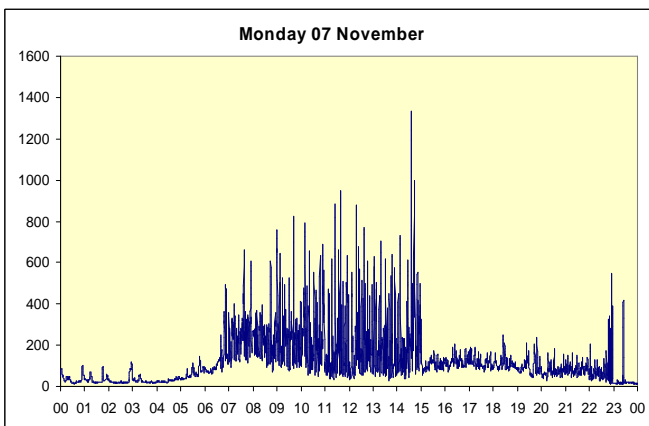
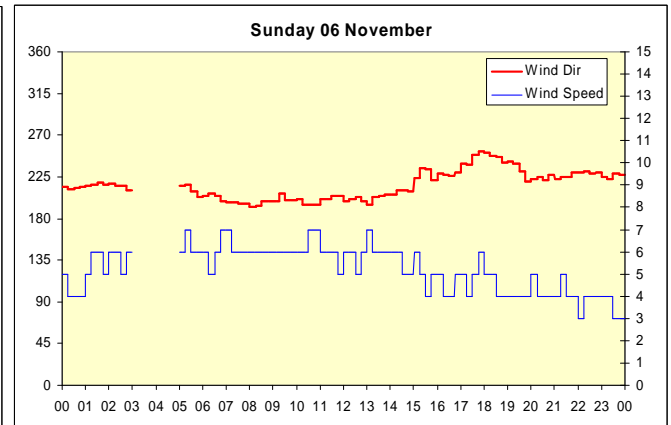
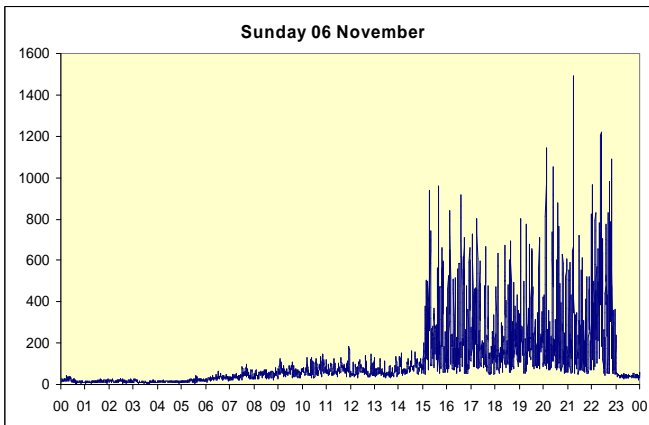
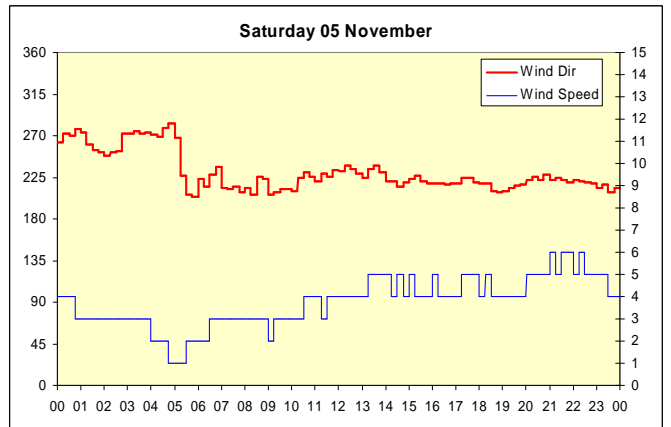
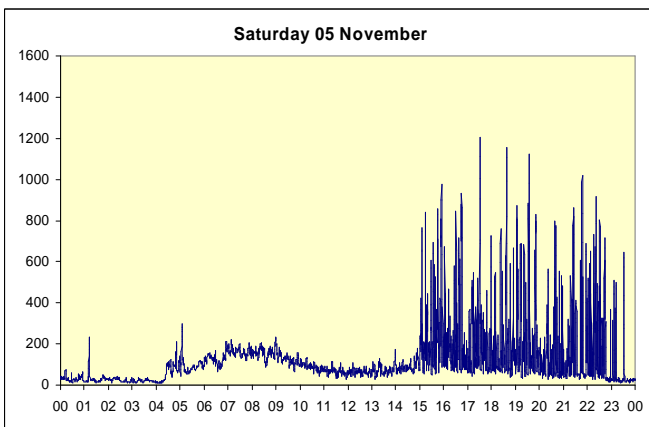
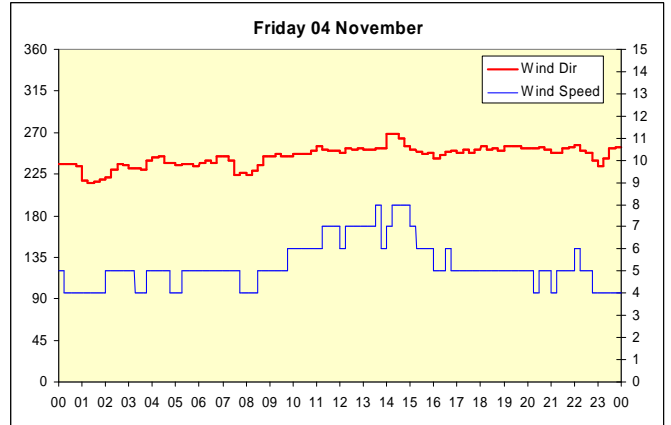
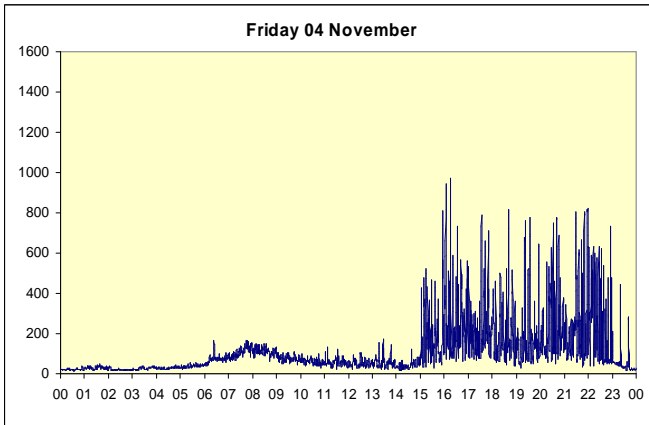
1. NO_x concentrations as 10-second values are shown in the following Figures for the full period 19 October to 15 November 2005, together with 15-minute wind data for the LHR2 site. All times are in GMT
2. Data from the 20 of the 28 days have been included in subsequent analyses, as follows: 19, 20, 21, 23, 24, 25, 26, 28, 30, 31 October and 1, 2, 3, 4, 5, 6, 7, 8, 10, 11 November 2005.

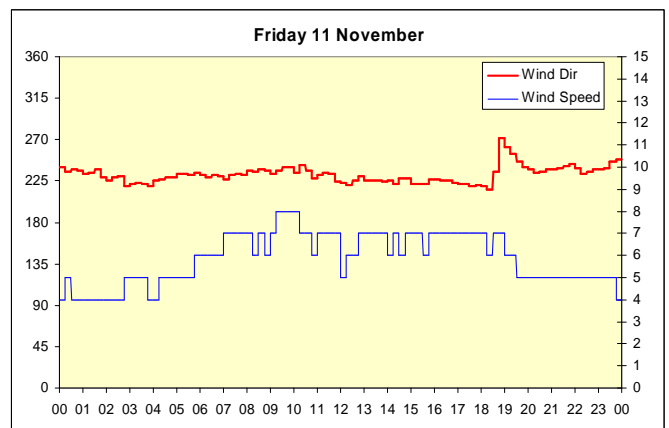
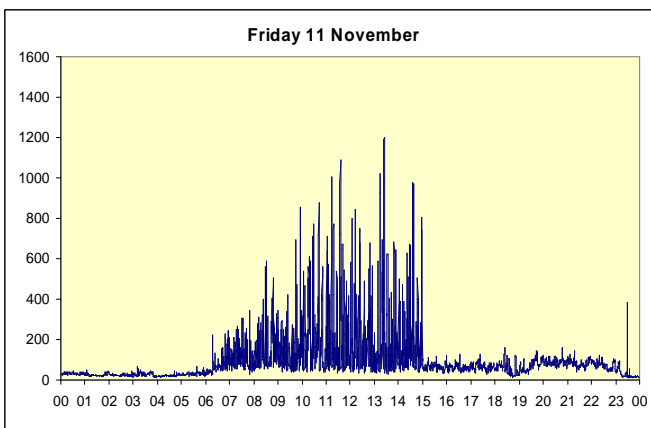
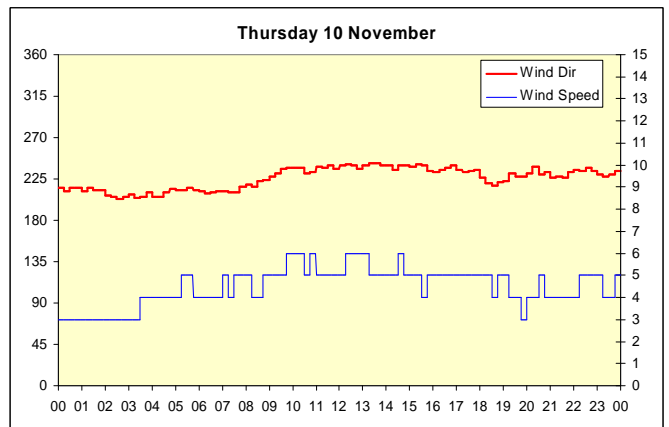
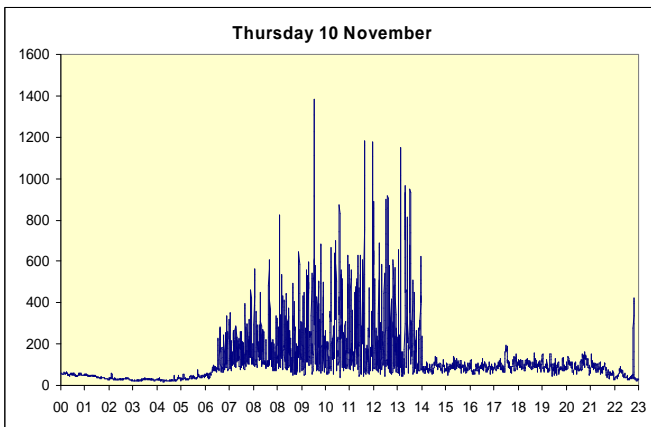
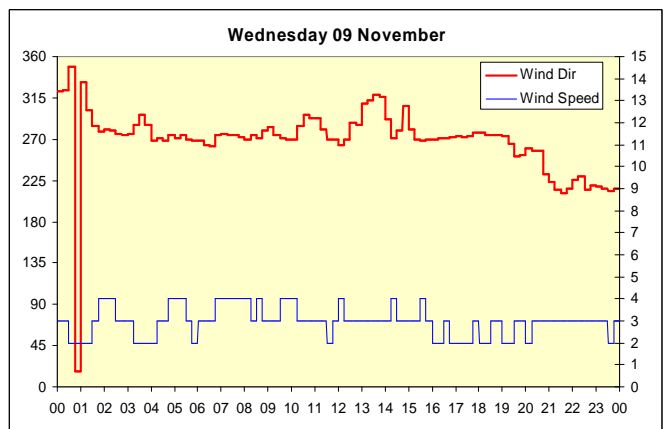
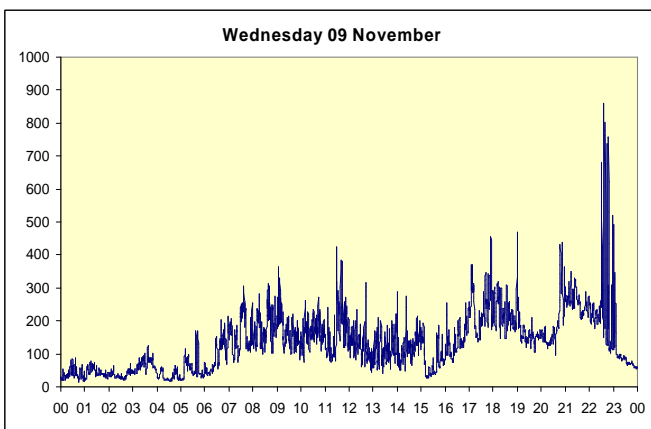
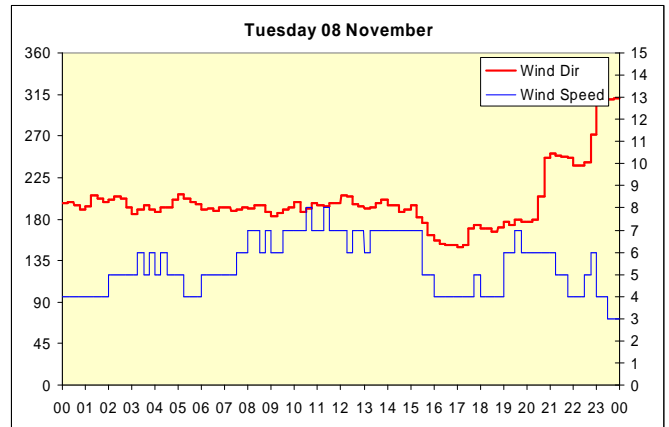
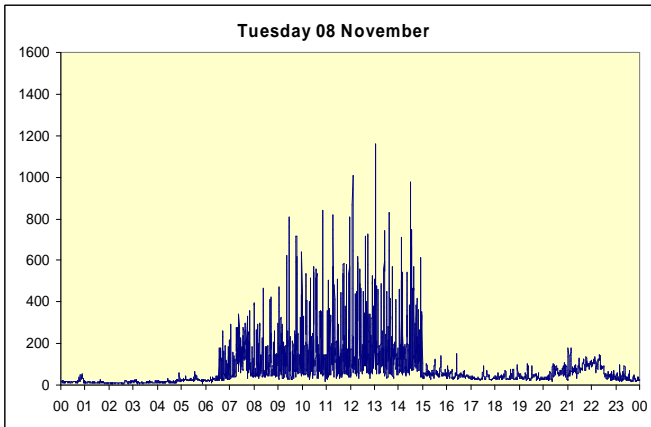


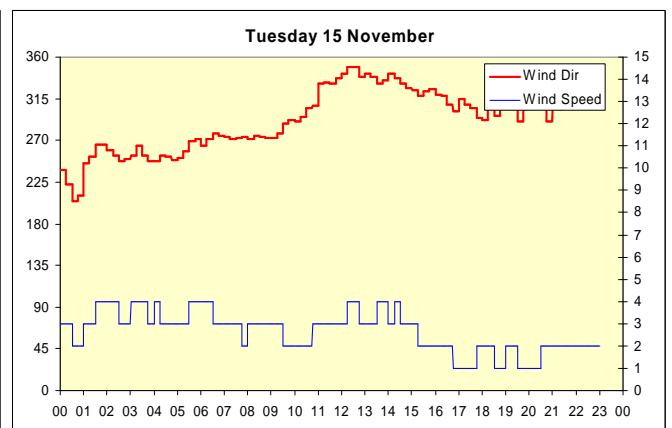
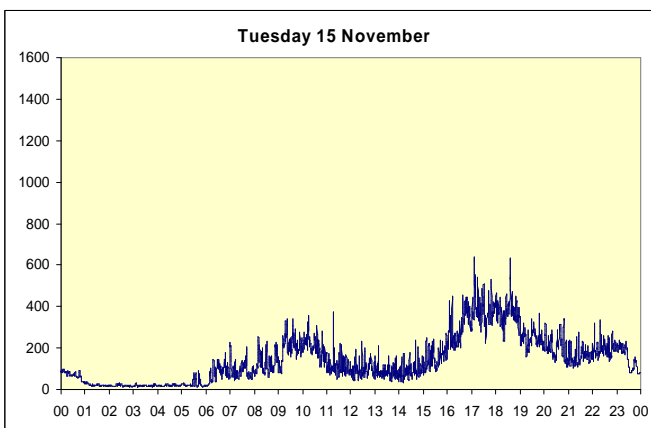
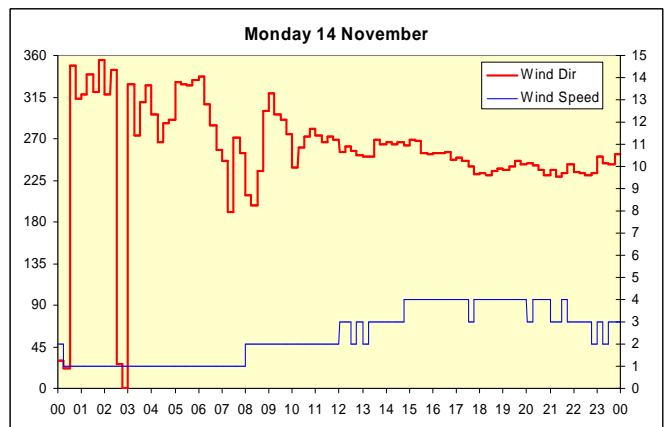
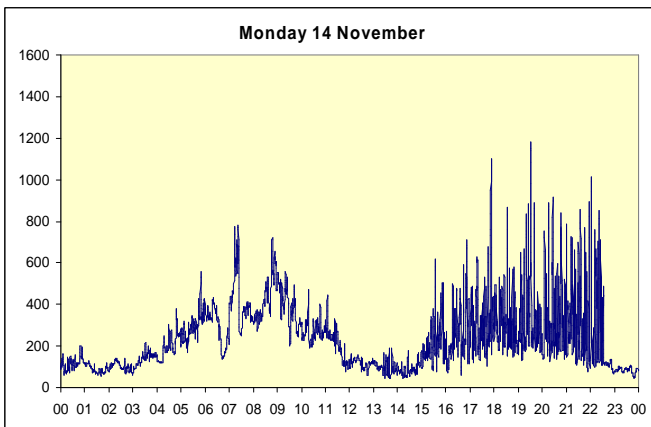
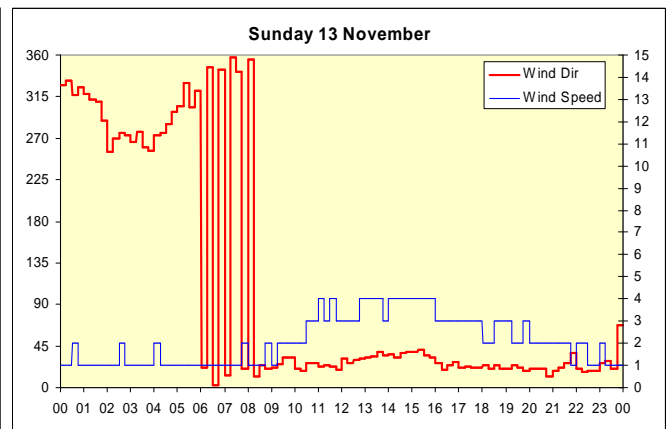
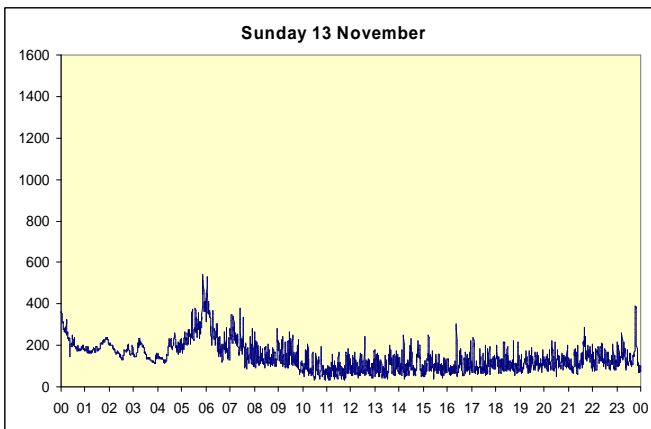
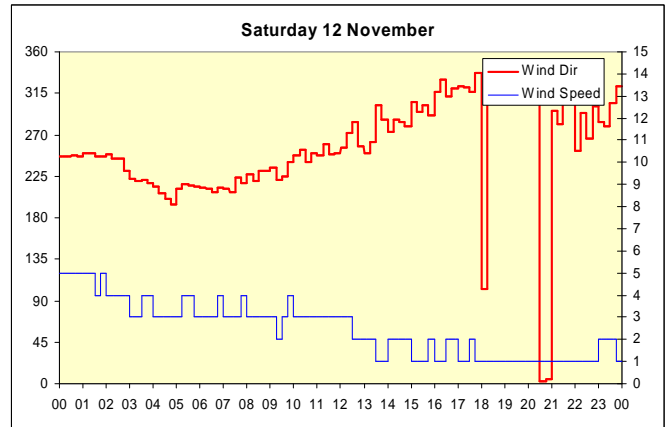
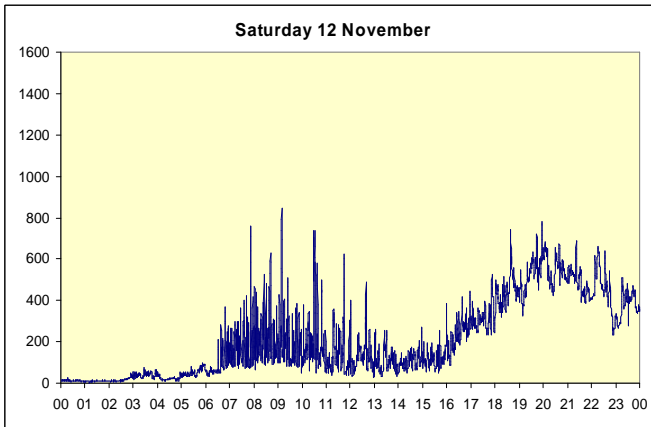












Appendix F – Daily Plots of 10-second NO_x Concentrations and Calculated Baseline at LHR2 and Measured Background at LHR8 (Oaks Road)

